Research report

BYTEC

Validation of test results on the numerical model of Sandwich beams

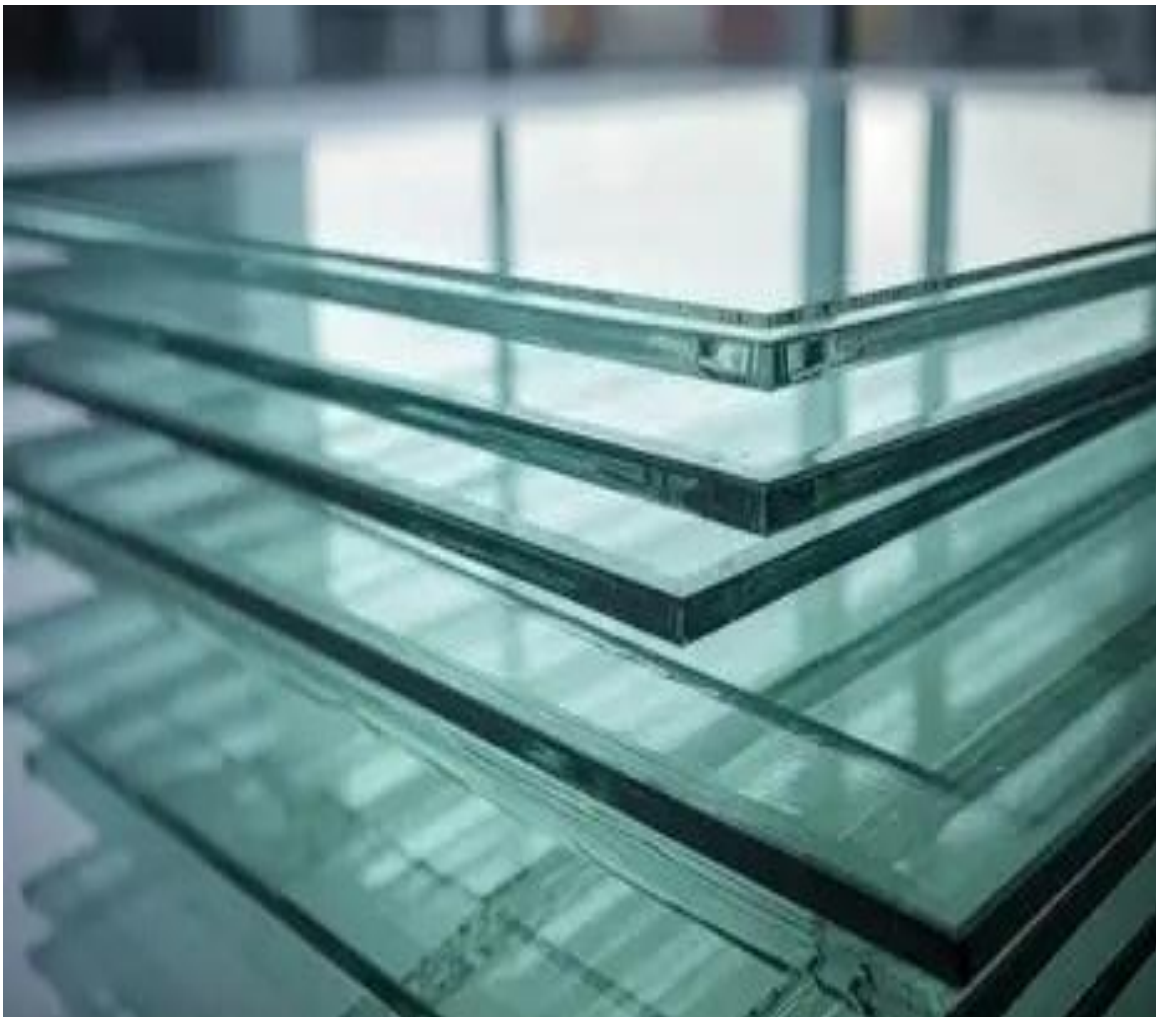

Report date: 04 May 2026 Hugo Sol

Contents

1 Introduction

This report describes some validation tests of the numerical model of symmetrical sandwich beam. The model can simulate static and dynamical responses. Static loads include 3- and 4-point bending. Dynamical responses include the computation of resonance frequencies and modal shapes.

The numerical model will be used for the identification of the transverse shear modulus of the polymer layer based on measured resonance frequencies of a test beam. The resonance frequencies of a free-free suspended sandwich beam will be measured using an impulse excitation technique. The vibration amplitudes of the test beam will be very small. This will allow assuming a small deformation theory and linear material behavior in the numerical model of the sandwich beam.

2 Validation of the model

2.1 Statical load cases

A simply supported sandwich beam is loaded in the middle with a concentrated transverse force P of 100 Newton (3-point bending).

The geometrical properties of the beam are:

Beam Length L:	0.3m
Beam Width W:	0.03m
Thickness of the 2 Glass Layers H:	0.002m
Thickness of the polymer Layer H_0:	0.003m

2.1.1 Validation case 1

For validation case 1 the Shear modulus G_0 and Young's modulus E_0 of the polymer layer have the same value of the glass moduli E and G:

Young's modulus Glass and polymer E = E_0:	7.E+10 N/m2
Poisson's ratio Glass and polymer:	0.22
Shear modulus Glass and polymer G=G_0:	2.48E+10 N/m2

With these assumptions, the sandwich laminate behaves like a solid beam with a thickness of 0.007m. The maximal deflection v of the beam and the beam stiffness can be calculated analytically:

$$EI = 60\ \mathrm{Nm}^2$$

$$v = \frac{PL^3}{48EI} = 0.000938\mathrm{m}$$

Figure 2.1.1.1 and 2.1.1.2 show the computed deflections and the different angles in the sandwich laminate.

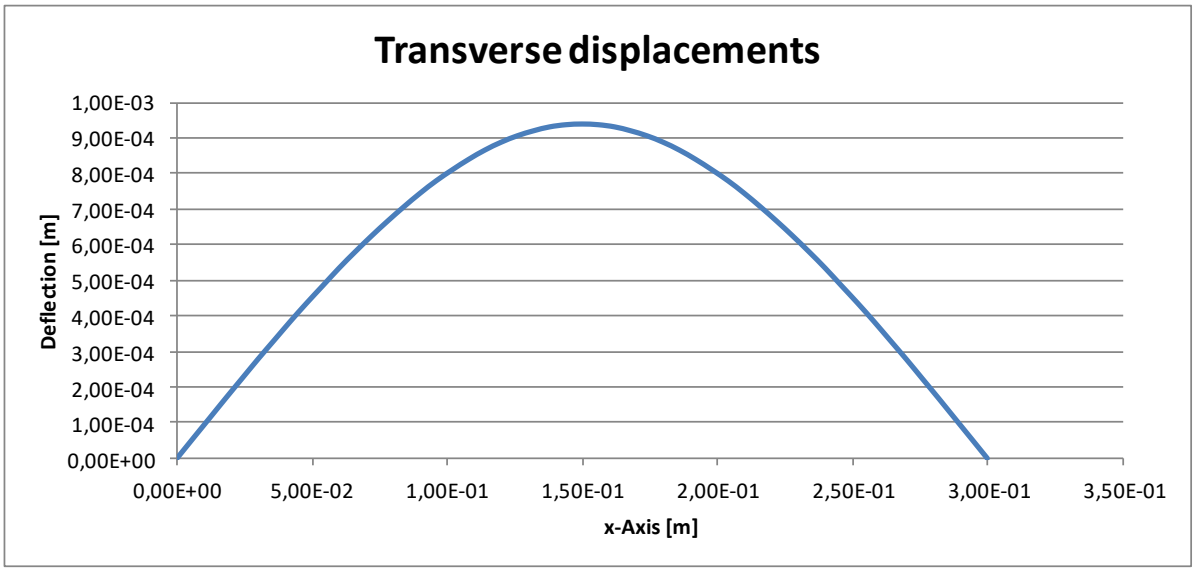

Figure 2.1.1.1 Computed deflections in the laminated sandwich in 51 points (solid glass)

The computed deflection in the middle of the beam = 0.000937m. The computed beam stiffness EI = 59.89 Nm2. This matches the analytical values nearly for 100%.

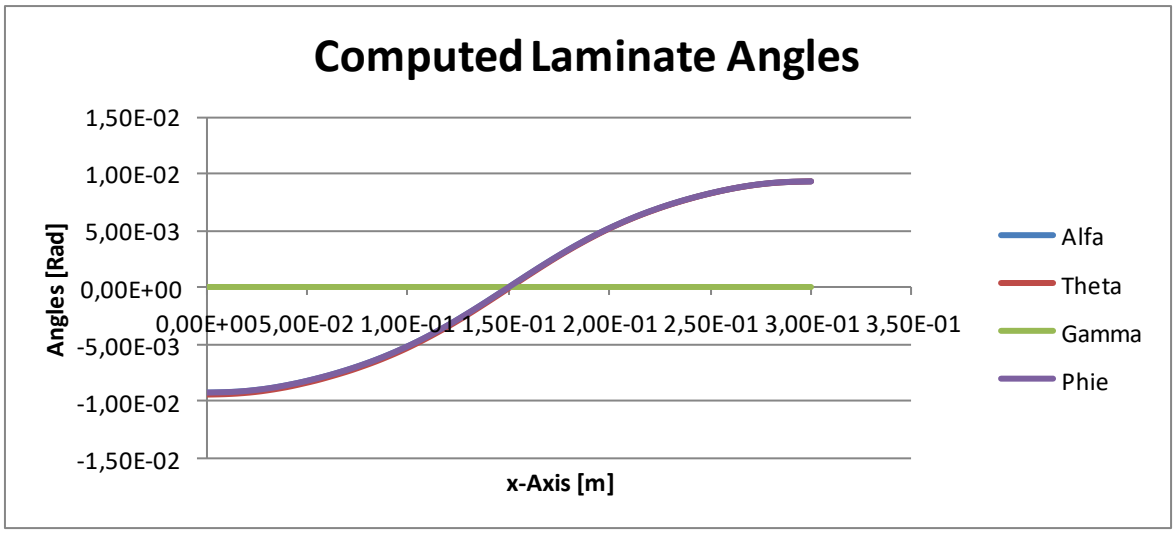

Figure 2.1.1.2 Computed angles in the sandwich laminate in 51 points (solid glass)

It can be observed that the angles Alfa, Theta and Phi are the same. The total shear angle Gamma = 0. This is in agreement with the theory (see internal report on theory model)

$$\varphi = \theta = \alpha$$

and

$$\gamma(x) = \varphi - \theta = 0$$

The maximal normal stress in the glass layer was computed as:

$$\sigma_x = 28.6 \text{ MPa}$$

This stress is about the maximal stress that glass can resist (between 10 MPa and 30 MPa, depending on the composition and treatment of the glass)

2.1.2 Validation case 2

For validation case 2 the Shear modulus G_0 and Young's modulus E_0 of the polymer layer are assumed to have a very low value:

Young's modulus polymer E_0: 10 N/m2
Shear modulus polymer G_0: 10 N/m2

With these assumptions, the 2 glass layers in the sandwich laminate will bend independently. The maximal deflection v of the beam and the beam stiffness can be calculated analytically:

$$EI = 2.8 \text{ Nm}^2$$

$$v = \frac{PL^3}{48EI} = 0.02009\text{m}$$

It is clear that the stiffness of the sandwich laminate is much lower as the previous solid beam case.

Figure 2.1.2.1 and 2.1.2.2 show the computed deflections and the different angles in the sandwich laminate computed in 51 internal points.

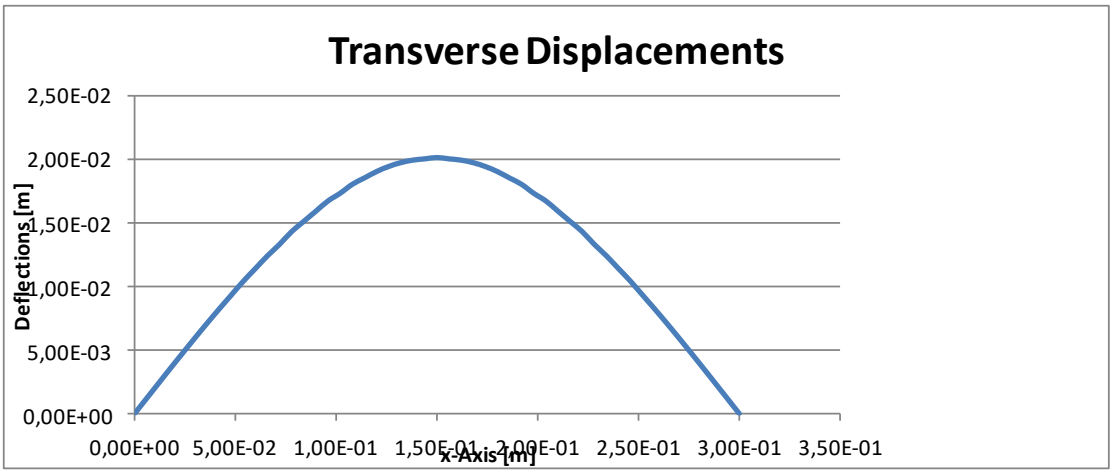

Figure 2.1.2.1 Computed deflections in the laminated sandwich in 51 points (independent bending)

The computed deflection in the middle of the beam = 0.02007m. The computed beam stiffness EI = 2.8 Nm2. This matches the analytical values nearly for 100%.

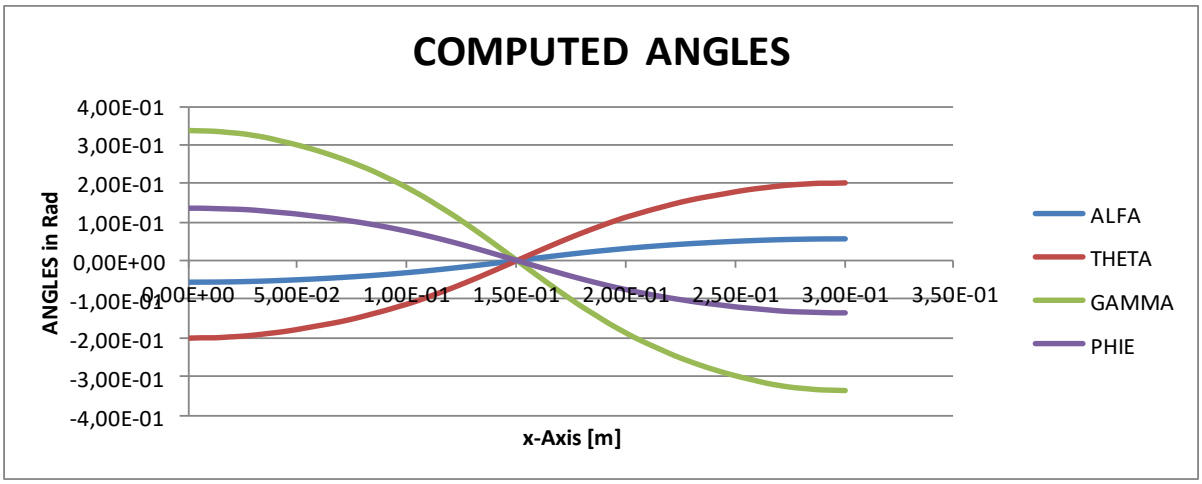

Figure 2.1.2.2 Computed angles in the sandwich laminate in 51 points (independent bending)

The maximal normal stress in the glass layer was computed as:

$$\sigma_x = 175 \text{ MPa}$$

This is much higher than the failure stress of glass.

Independent bending of the layers makes the laminate much more flexible (20 times more flexible than solid glass of the same thickness) and generates much higher stresses in the glass.

2.1.3 Example with PVB layer

This example studies a laminate with a PVB layer with low modulus G_0 and Young's modulus E_0 .

Young's modulus of PVB E_0:	2.E+08 N/m^2
Poisson's ratio PVB:	0.45
Shear modulus PVB G_0:	0.69E+08 N/m^2

Figure 2.1.3.1 and 2.1.3.2 show the computed deflections and the different angles in the sandwich laminate.

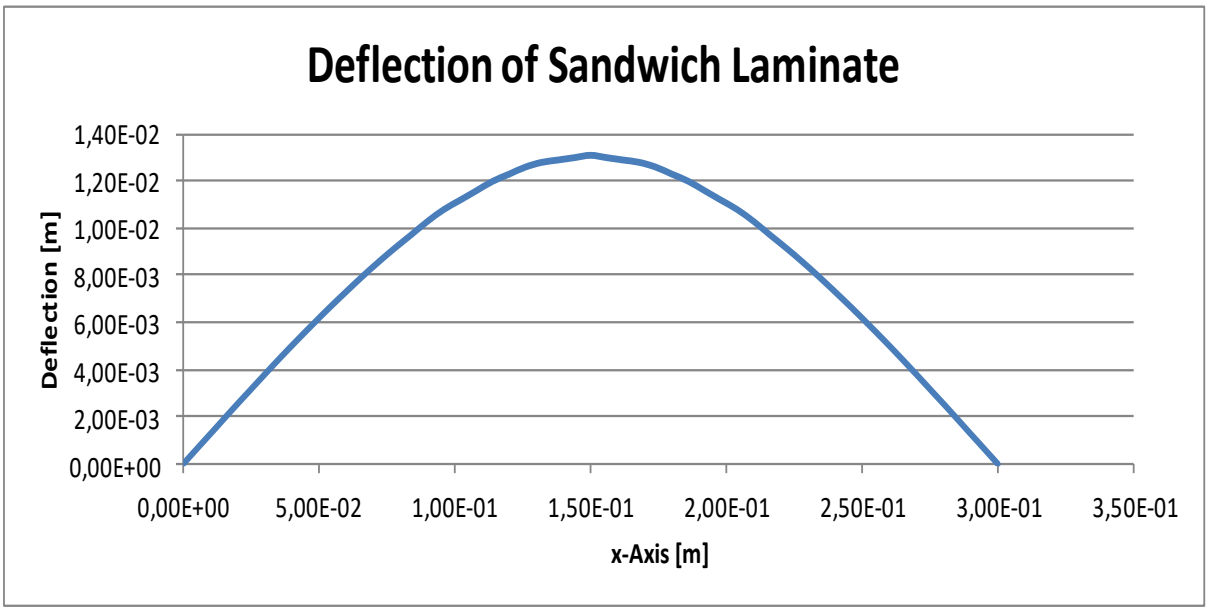

Figure 2.1.3.1 Computed deflections in the laminated sandwich in 51 points (PVB layer)

The maximal deflection in the middle is 0.01307m.

The maximal normal stress in the glass layer was computed as:

$$\sigma_x = 127 \text{ MPa}$$

This is much higher than the failure stress of glass.

This example with the PVB layer is hence close to the extreme case of the independent bending of the glass layers.

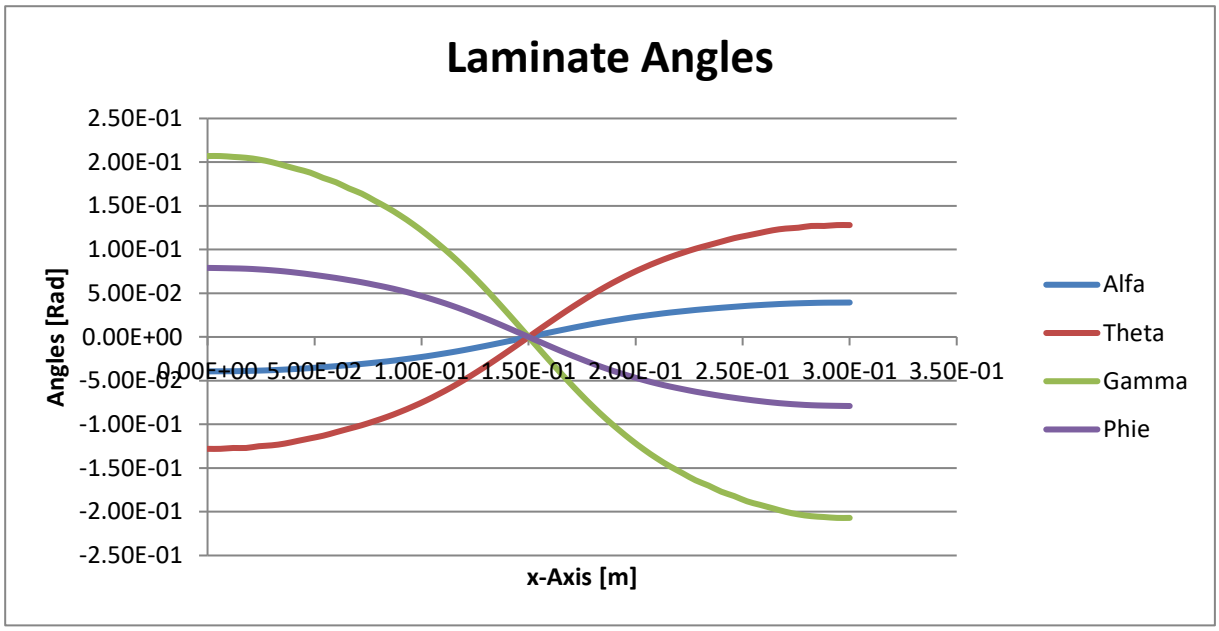

Figure 2.1.3.2 Computed angles in the sandwich laminate in 51 points (PVB layer)

The equivalent beam stiffness $(EI)_{Equivalent}$ can be computed as:

$$(EI)_{Equivalent} = \frac{PL^3}{48v} = 4.3Nm^2$$

This value is close to the minimal stiffness of the laminate of $2.8Nm^2$ (independent glass layer bending) and very far from the maximal stiffness of $59.9Nm^2$ (if the laminate behaves as a solid glass beam).

2.1.4 Validation of result with finite element simulations

The previous test case with the PVB layer is simulated in a finite element program using 2D plane stress elements.

2.1.4.1 Validation with fully integrated linear elements

The two glass layers and the PVB layer were modeled with linear 4 node elements. The table 2.1.4.1.1 shows the result of simulations with an increasing number of elements.

Total number of elements	Number of elements in the glass layer	Number of elements in the PVB layer	Maximal computed displacement	Computed displacement with current numerical model
1005	1	2	0.01110	0.01307
4011	3	4	0.01270	0.01307
9015	4	6	0.01290	0.01307
14269	5	8	0.01304	0.01307
25025	7	10	0.01311	0.01307
34829	8	12	0.01313	0.01307
54036	10	15	0.01316	0.01307
94047	15	20	0.01319	0.01307

Table 2.1.4.1.1 Comparison between current model and linear finite element simulations

The finite element results converge to the value 0.01319 with nearly 100,000 elements. This is 0.5% more than the numerical model used in this report. The 0.5% higher value can be explained because the finite element model takes also the transverse shear deformation of the glass layer into account.

The figure 2.1.4.1.1 shows a snap shot of the finite element output of the normal stresses. It can be clearly noticed that the two glass layers are bending individually (tensile stress in the upper layer and compressive stress in the lower layer). This confirms that the laminate with the PVB layer is close to the limit state in which the glass layers are bending individually.

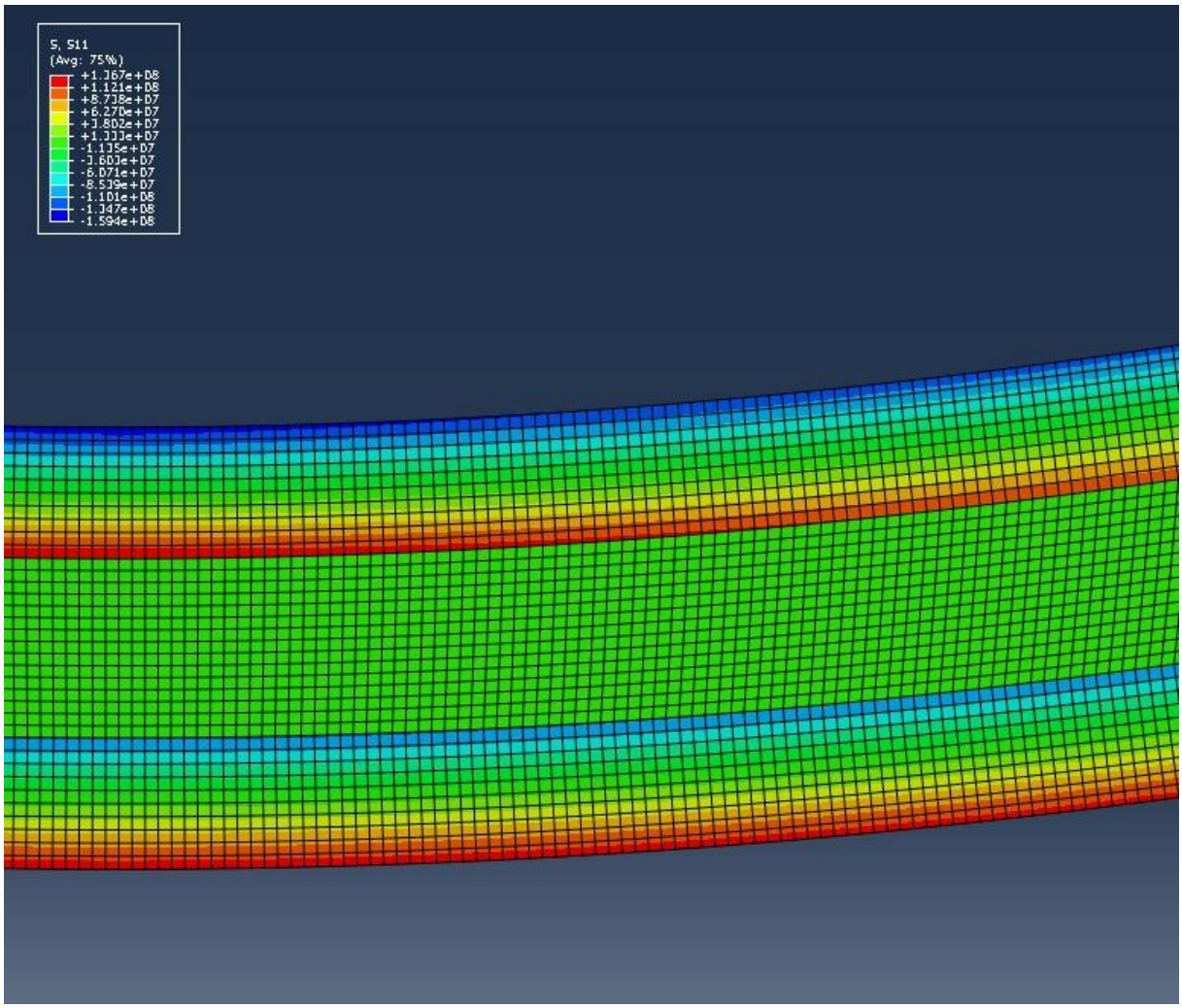

Figure 2.1.4.1.1. Zoom on the normal stress output of the finite element model (case 54036 elements)

(computed with the finite element program ABAQUS)

2.1.4.2 Validation with quadratic elements

Because fully integrated linear elements have a poor convergence for bending (shear locking), the same laminate was also modeled with quadratic elements:

Number of elements in the FE model	Maximal computed FE displacement	Computed displacement with the current model
227	0.01317	0.01307
2809	0.01319	0.01307

Table 2.1.4.2.1 Comparison between current model and quadratic finite element simulations

The 0.5% higher value can be explained because the finite element model takes also the transverse shear deformation in the glass layer into account.

2.1.5 Validation of 4 point bending case

The test sandwich beam has following characteristics:

- Length L = 300 mm
- Thickness skin h: 3.35 mm
- Thickness core h0: 40.3 mm
- Sandwich thickness t: 47.0 mm
- Density skin: 1712 kg/m3
- Density core: 193 kg/m3
- Young's modulus skin: 17300 MPa
- Young's modulus core: 184 MPa
- Transverse shear modulus: 52.1 MPa

4 point bending distance to loads: 72.5 mm,
distance between load points: 155 mm
total load: 2 x (1 x 5) = 10 N

Figure 2.1.5.1 show the deflection of the sandwich computed by the FE program ABAQUS using 2D in-plane elements (unity width = 1)

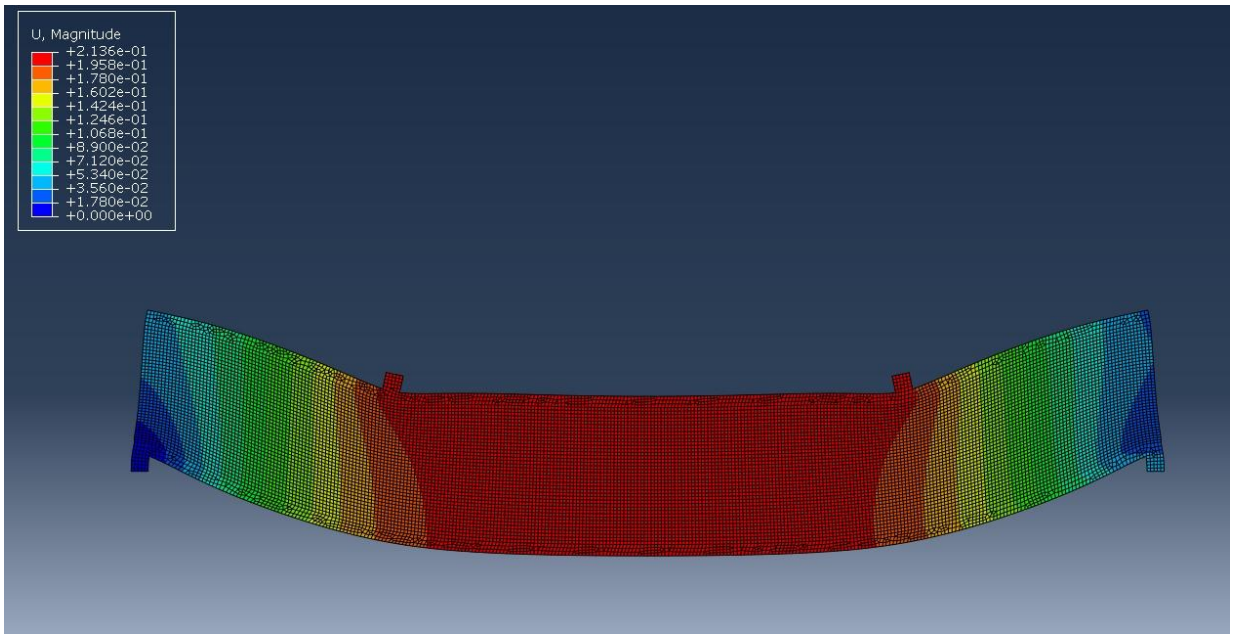

Figure 2.1.5.1. Deflection computed by the finite element model

Maximal Deflection ABAQUS	Maximal deflection current model
0.213 mm	0.219 mm

Table 2.1.5.1 Comparison between current model and finite element simulations

The following figure 2.1.5.2 shows the strain in the longitudinal direction. The top layer is loaded in compression (blue), while the bottom layer is loaded in tension (red).

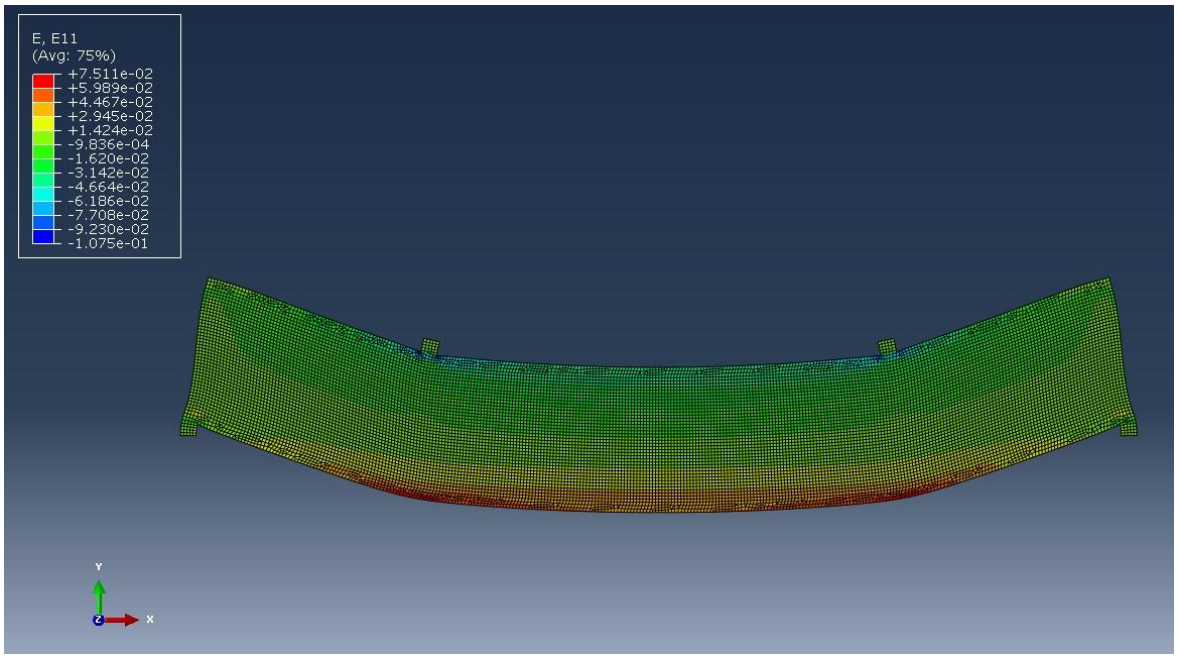

Figure 2.1.5.2. Strain in the longitudinal direction

Figure 2.1.5.3 shows the strain in the transverse direction.

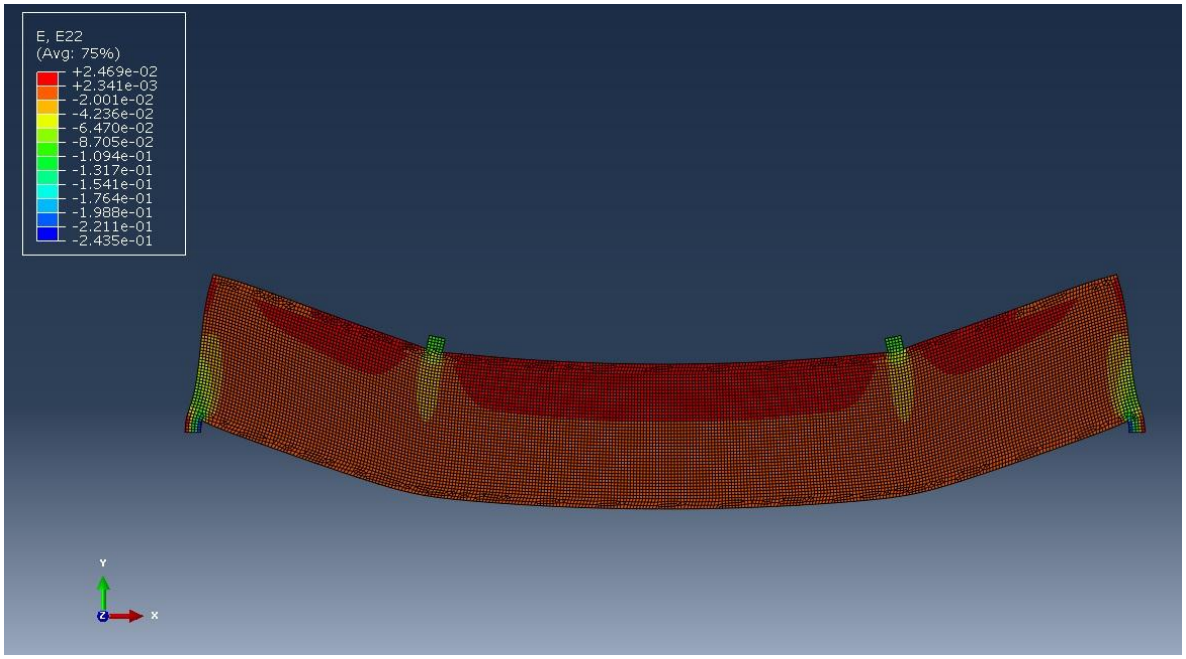

Figure 2.1.5.3. Strain in the transverse direction

It can be seen that the transverse strain is in tension. This is the reason why the top layer of a sandwich delaminates in the top layer when load heavely.
The next figure 2.1.5.4 shows the normal stress distribution.

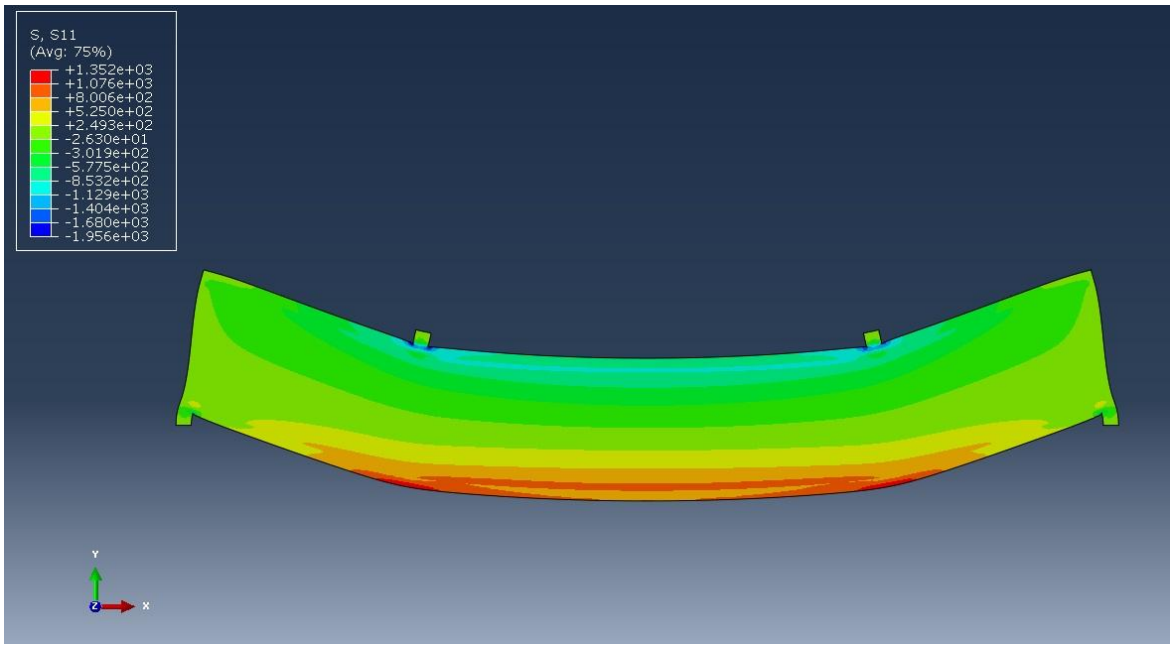

Figure 2.1.5.4. Normal stress distribution

Figure 2.1.5.5 shows the shear stress distribution.

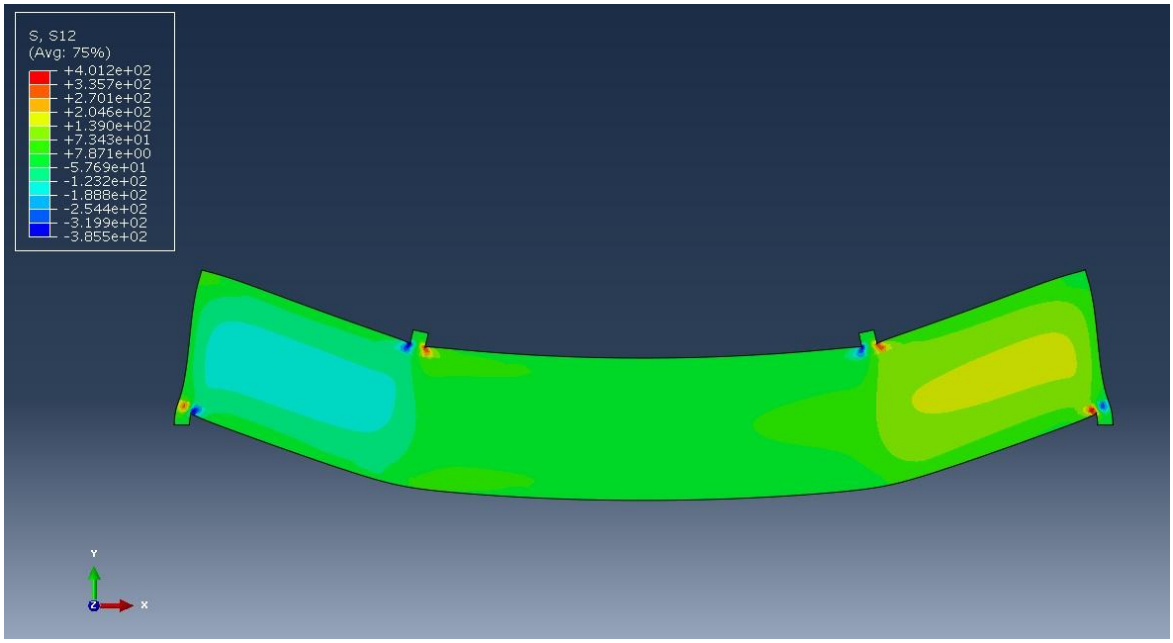

Figure 2.1.5.5. Shear stress distribution

It can be observed that the shear stress between the loading points is zero.

2.2 Computation of the Natural Frequencies

2.2.1 Test case 1: glass/PVB/Glass laminate

The fundamental natural frequency of a free-free sandwich beam is computed for several values of the elastic Young's and Shear modulus of the polymer.

The geometrical properties of the beam are chosen as:

Beam Length L:	0.25m
Beam Width W:	0.01m
Thickness of the 2 Glass Layers H:	0.003m
Thickness of the polymer Layer H_0:	0.006m
Specific Mass of the Glass Layerρ:	2600 kg/m^3
Specific Mass of the Polymer Layerρ_0:	1000 kg/m^3

The resonance frequencies of the free-free beam are computed with the numerical model and with a finite element model. The finite element was built with (3 x 3 x 25) = 225 three dimensional PR- elements. Each element has 21 nodal points (PR-21).

The equivalent stiffness of the beam EI (considered as an Euler Bernoulli beam) can be computed with the obtained frequency f and the cross section areas A and A_0:

$$(EI)_{Equivalent} = \frac{4\pi^2 L^4(\rho_0 A_0 + \rho A)f^2}{501}$$

The Young's modulus and Shear modulus of the polymer layer varies between the properties of the glass till a E+05 times smaller value.

The computed resonance frequencies and the total bending stiffness according to formula are listed in the next table. An example of a computed mode shape with the finite element model is shown in figure 2.2.1.1.

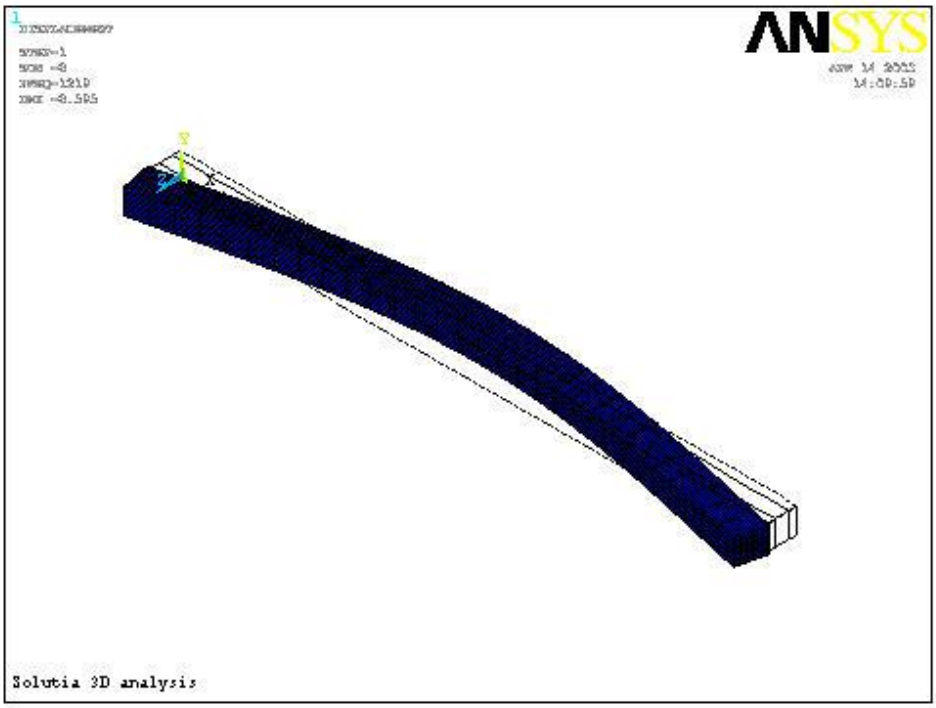

Figure 2.2.1.1. Modal shape associated with the fundamental natural frequency

(computed with the finite element program ANSYS)

Case Nr.	E-Modulus Polymer [Pa]	G-Modulus Polymer [Pa]	F_{ANSYS} [Hz]	$F_{Num.Model}$ [Hz]	Equivalent Stiffness [Nm^2]
1	7.E+10	2.69E+10	1219	1216	99.5
2	7.E+09	2.69E+09	1127	1124	84.9
3	7.E+08	2.69E+08	960	958	61.7
4	7.E+07	2.69E+07	542	542	21.6
5	7.E+06	2.69E+06	282	282	5.8
6	7.E+05	2.69E+05	225	225	3.7
7	7.E+04	2.69E+04	218	218	3.2

Table 2.2.1.1 Fundamental natural frequencies and equivalent stiffness values

It can be observed that the values of the frequencies computed with the numerical model are in perfect agreement with the finite element simulations.

The first case gives the stiffness of a monolith glass beam, while case 7 gives the situation for low polymer stiffness. It can be observed that the equivalent stiffness of the laminate in case 1 is about 30 times bigger as for the case 7. The situation for a PVB beam in test case 3 (G-modulus 6.9E+05) is between case 5 and 6.

Figure 2.2.1.2 compares the equivalent stiffness of the laminate with the stiffness of a monolith glass beam of 12mm and 6mm thickness.

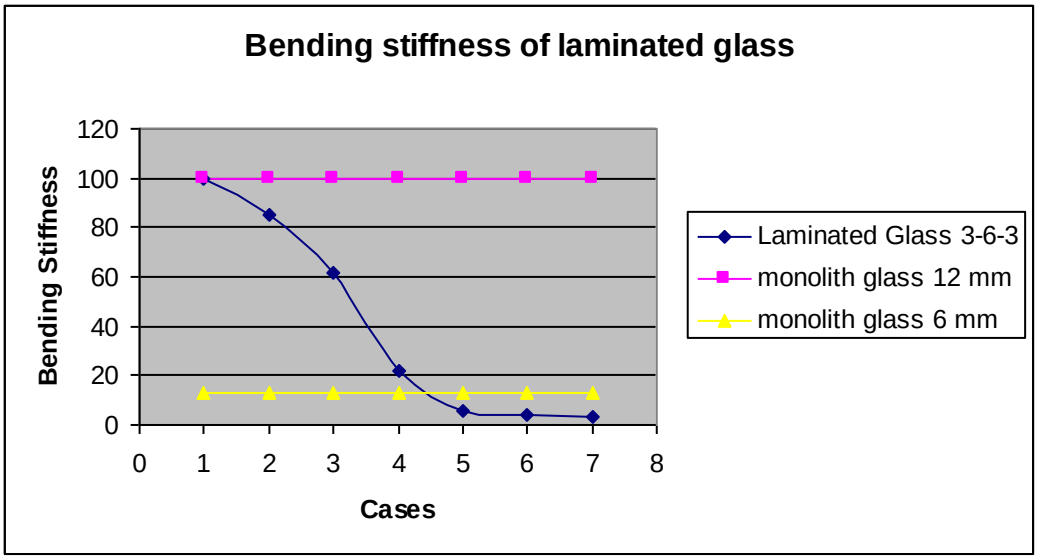

Figure 2.2.1.2. Bending stiffness of laminated glass

2.2.2 Test case 2: Sandwich with very thin skins

A sandwich beam with face sheets made from glass fibre reinforced plastics (GFRP) and a core layer made from PVC foam is studied in detail in [2]. The resonance frequencies are derived from wave propagation equations. The results from the proposed sandwich finite element model are compared with those from wave propagation model. The properties of the sandwich beam are listed in Table 2.2.2.1. The boundary condition is free-free. The calculated resonance frequencies both from [2] and from current study, the measured frequencies, and the corresponding relative errors are listed in Table 2.2.2.2.

	Density (kg/m3)	E modulus (Pa)	Thickness (m)	Length (m)	Width (m)	Poisson's ratio
GFRP	1580	9.80e9	2.5e-3	1.65	116e-3	0.3
PVC	101	9.40e7	50e-3	1.65	116e-3	0.3

Table 2.2.2.1. Properties of sandwich beam

Frequency Number	Results Current model [Hz]	Results FE Model [1] [Hz]	Results Model [2] [Hz]	Experiments In [2] [Hz]
1	65	64	65	62
2	164	161	161	161
3	289	283	288	288
4	426	413	428	428

Table 2.2.2.2. Resonance frequencies comparison

From Table 2.2.2.2, the following conclusion can be drawn:

(1) by comparing the current results with those calculated in [1] it is clear that both the current sandwich finite element model and the wave propagation model are very close to each other;

(2) by comparing the calculated results with experimental results in [2] it can be seen that the all results have a minor difference as compared with the experimental results. This discrepancy results from the inaccurate input material properties in Table 2.2.2.1. In [2], the E-modulus of the GFRP face sheet and G-modulus of the PVC core are measured as follows:

- First, the GFRP face sheet is measured separately. The face sheet is suspended by using very soft cord to simulate the free-free boundary condition. The E-modulus is calculated from the measured frequencies using Euler's formula of a free-free beam vibration.
- Secondly, a beam made with only the PVC core is measured separately. The resonance frequencies are measured similarly as in [1]. The E modulus is calculated again from the resonance frequencies using Euler's formula. By using the formula of isotropic material ($G=E/2(1+\mu)$) and assuming a value of Poisson's ratio equal to 0.3, the shear modulus G is calculated.

It is clear that the input E modulus of the GFRP face sheets and the G modulus of the PVC core not very accurate. Several influence factors are not taken into account during the course of deriving the E modulus and the G modulus:

- for the thick, soft PVC core, Euler's beam free-free vibration formula is not accurate because of the influence of the transverse shear modulus
- The material properties of the face sheets and the core are different before and after their assemblage into the sandwich beam. The influence of the adhesive layer between the face sheets and the core in sandwich beams cannot be ignored. This is exactly the reason why a more accurate, convenient way is needed to identify the material properties of the sandwich beam instead of measuring them separately
- The shear modulus of the core is calculated from an assumed Poisson's ratio of 0.3. This results in an inaccurate shear modulus.

With corrected values found in [1], new values for the resonance frequencies closer to the measured values, could be found (see table 2.2.2.3)

	E-Modulus [Pa]	**Shear Modulus [Pa]**
GFRP	9.216E+9	4.494E+7

Frequency Number	**Results Current model [Hz]**	**Results FE Model [1] [Hz]**	**Experiments In [2] [Hz]**
1	62.4	62.8	62
2	161	161	161
3	288	287.4	288
4	428	427.9	428

Table 2.2.2.3. Resonance frequencies comparison

2.2.2.1 References

[1] Material parameter identification of sandwich beams by an inverse method, Yinming Shi, Hugo Sol, Hongxing Hua, Department of Mechanics of Material and Construction, Vrije Universiteit Brussel, Brussels, Belgium, Journal sound and vibrations, Volume 290, Issues 3–5, 7 March 2006, Pages 1234-1255

[2] S. S. Tavalaelly, *Wave Propagation in Sandwich Structures*, PhD Thesis, Department of Vehicle Engineering, The Marcus Wallenberg Laboratory for Sound and Vibration Research, Stockholm, 2001.

2.2.3 Test case 3: Example with PVB layer

The fundamental natural frequency of the same PVB sandwich beam as in the static example case 3 is computed.

The geometrical properties of the beam are:

Beam Length L:	0.25m
Beam Width W:	0.01m
Thickness of the 2 Glass Layers H:	0.003m
Thickness of the polymer Layer H_0:	0.006m
Specific Mass of the Glass Layerρ:	2600 kg/m^3
Specific Mass of the Polymer Layerρ_0:	1000 kg/m^3

This example studies a laminate with a PVB layer with modulus G_0 and Young's modulus E_0 .

Young's modulus of PVB E_0:	2.E+08 N/m^2
Poisson's ratio PVB:	0.45
Shear modulus PVB G_0:	0.69E+08 N/m^2
Young's modulus Glass E :	7.E+10 N/m2
Poisson's ratio Glass:	0.22
Shear modulus Glass G:	2.48E+10 N/m2

2.2.3.1 Equivalent stiffness

The equivalent stiffness of the beam EI (considered as an Euler Bernoulli beam) is computed with the obtained frequency f and the cross section areas A and A_0 using (73):

$$(EI)_{Equivalent} = \frac{4\pi^2 L^4(\rho_0 A_0 + \rho A)f^2}{501}$$

The beam stiffness of a monolithic glass beam with the same thickness $2h + h_0$ as the laminate can be computed as:

$$(EI)_{Monolith} = \frac{Eb(2h+h_0)^3}{12}$$

2.2.3.2 Normal stresses in the glass layers

If the modal shape of the first natural frequency is considered as "frozen" in an arbitrary position, the stresses in the glass layer can be computed from the bending moment in the glass layer and the normal force in the glass layer. The maximal bending moment and normal force will occur in the Middle node of the beam model.

$$(M_{Glass})_{Mid\ Node} = \frac{Ebh^3}{12}\left(\frac{\partial^2 w}{\partial x^2}\right)_{Mid\ Node}$$

$$(N)_{Mid\ Node} = Ebh\left[\frac{(2h+h_0)}{2}\left(\frac{\partial \alpha}{\partial x}\right)_{Mid\ Node} + \frac{h}{2}\left(\frac{\partial^2 w}{\partial x^2}\right)_{Mid\ Node}\right]$$

The maximal normal stress in the frozen position can be computed as the summation of the stress induced by the bending moment and the stress induced by the normal force.

$$(\sigma)_{Mid\ Node} = \frac{6(M_{Glass})_{Mid\ Node}}{bh^2} + \frac{(N)_{Mid\ Node}}{bh}$$

This normal stress in the glass layer can be compared with the stress induced in a monolithic glass beam with the same thickness $2h + h_0$ as the laminate.

$$(\sigma)_{Monolith} = \frac{12(M_{total})_{Mid\ Node}}{bh^2}$$

The total bending moment in the Middle node of the model can be computed by integration of the inertia forces of a free-free Euler Bernoulli beam vibrating in resonance at a circular frequency ω.

The inertia forces causing transverse shear forces and bending moments in the beam sections are the second term in the time independent equilibrium differential equation describing the modal shape W(x) of a vibrating beam:

$$\frac{d^2}{dx^2}\left(EI\frac{d^2W(x)}{dx^2}\right) - W(x)\left(\rho_0 A_0 + \rho A\right)\omega^2 = 0$$

This equation can be seen as the differential equation of a beam loaded statically with a distributed pressure $p(x) = W(x)(\rho_0 A_0 + \rho A)\omega^2$. The pressure distribution is such that the load causes no rigid body translation or

rotation. This is obvious as the origin of the pressure distribution is a modal shape of a free-free beam. Equation (79) can hence be rewritten as:

$$\frac{d^2}{dx^2}\left(EI\frac{d^2W(x)}{dx^2}\right) = p(x)$$

Integration of this equation yields:

$$\frac{d}{dx}\left(EI\frac{d^2W(x)}{dx^2}\right) = \int_0^x p(\delta)d\delta = Q(x)$$

Q(x) is the transverse shear force at position x. In case of a free-free beam with length L, the shear force is zero at the beam boundaries x=0 and x=L.

Integration of the differential equation yields:

$$EI\frac{d^2W(x)}{dx^2} = \int_0^x Q(\delta)d\delta = M(x)$$

M(x) is the bending moment at position x. In case of a free-free beam with length L, the bending moment is zero at the beam boundaries x=0 and x=L.

The value of the total bending moment in the middle of the beam $(M_{total})_{Mid\ Node}$ can be found by evaluating M(x) in the middle of the beam.

The ratio between the normal stress computed in the glass layer and the normal stress in the monolithic beam gives the stress ratio of the beam. It can be assumed that the glass layers take all the stresses. This means the stress ratio is also the strength ratio of the laminate compared with a monolithic glass beam.

$$\text{Stress ratio} = \text{Strength ratio} = \frac{(\sigma)_{Monolith}}{(\sigma)_{Mid\ Node}}$$

2.2.3.3 Results for the PVB beam

RESULTS OF THE EIGENVALUE CALCULATIONS

NO	EIGENFREQUENCY
1	128.962943593252
2	306.099126701196
3	583.267619886972
4	952.979577962030

EIGENVALUE= 6.56583E+05 ACCURACY= 3.32010E-07

EIGENVECTOR COMPONENTS:

5.6650
26.269
3.1042
26.226
.60986
24.274
-1.5455
18.979
-3.0201
10.457
-3.5453
-1.16183E-06
-3.0201
-10.457
-1.5455
-18.979
.60987
-24.274
3.1042
-26.226
5.6650
-26.269

EIGENVALUE= 3.69900E+06 ACCURACY= 2.43328E-07

EIGENVECTOR COMPONENTS:

-5.6964
-71.780
-1.3185
-69.344
2.2721
-55.337
3.8216
-30.987
2.7982
-7.8007
4.84891E-05
1.6807
-2.7981
-7.8004
-3.8215
-30.986
-2.2721
-55.336
1.3184
-69.344
5.6963
-71.779

EIGENVALUE= 1.34306E+07 ACCURACY= 8.88955E-07

EIGENVECTOR COMPONENTS:

5.7784
61.706
-.23602
52.559
-3.6926
11.969
-2.3199
-32.644
1.8517
-37.506
4.0596
2.13658E-08
1.8517
37.506
-2.3199
32.644
-3.6926
-11.969
-.23602
-52.559
5.7784
-61.706

EIGENVALUE= 3.58531E+07 ACCURACY= 5.63465E-08

EIGENVECTOR COMPONENTS:

5.8284
135.68
-1.8000
113.55
-3.4600
29.742
1.4437
6.5801
3.8372
66.337
2.97837E-05
106.99
-3.8371
66.338
-1.4437
6.5806
3.4600
29.742
1.8000
113.55
-5.8283
135.68

&&& SECTION FORCES OUTPUT FIRST MODE

	SHEAR FORCE	BENDING MOMENT
1	.00000	.00000
2	34726.	571.59
3	49315.	1881.7
4	45273.	3343.3
5	26643.	4451.3
6	-34.769	4860.9
7	-26712.	4449.2
8	-45343.	3339.1
9	-49385.	1875.4
10	-34795.	563.25
11	-69.532	-10.430

MAX GLASS MOMENT: 1661.0 Nm
MAX GLASS NORMAL FORCE: 3.09734E+05 N
STRENGTH RATIO: .22491

EQUIVALENT STIFFNESS VALUE: 4.2674 Nm^2
STIFFNESS MONOLITH: 60.025 Nm^2

It can be verified that the equivalent stiffness value and the monolith stiffness are indeed the same as in the static cases (2.1.1) and (2.1.3).

2.2.3.4 Validation with Finite Elements

The beam was simulated in ABAQUS using 800 quadratic plain stress elements.

The figures below show the first 4 eigenvectors (modal shapes)

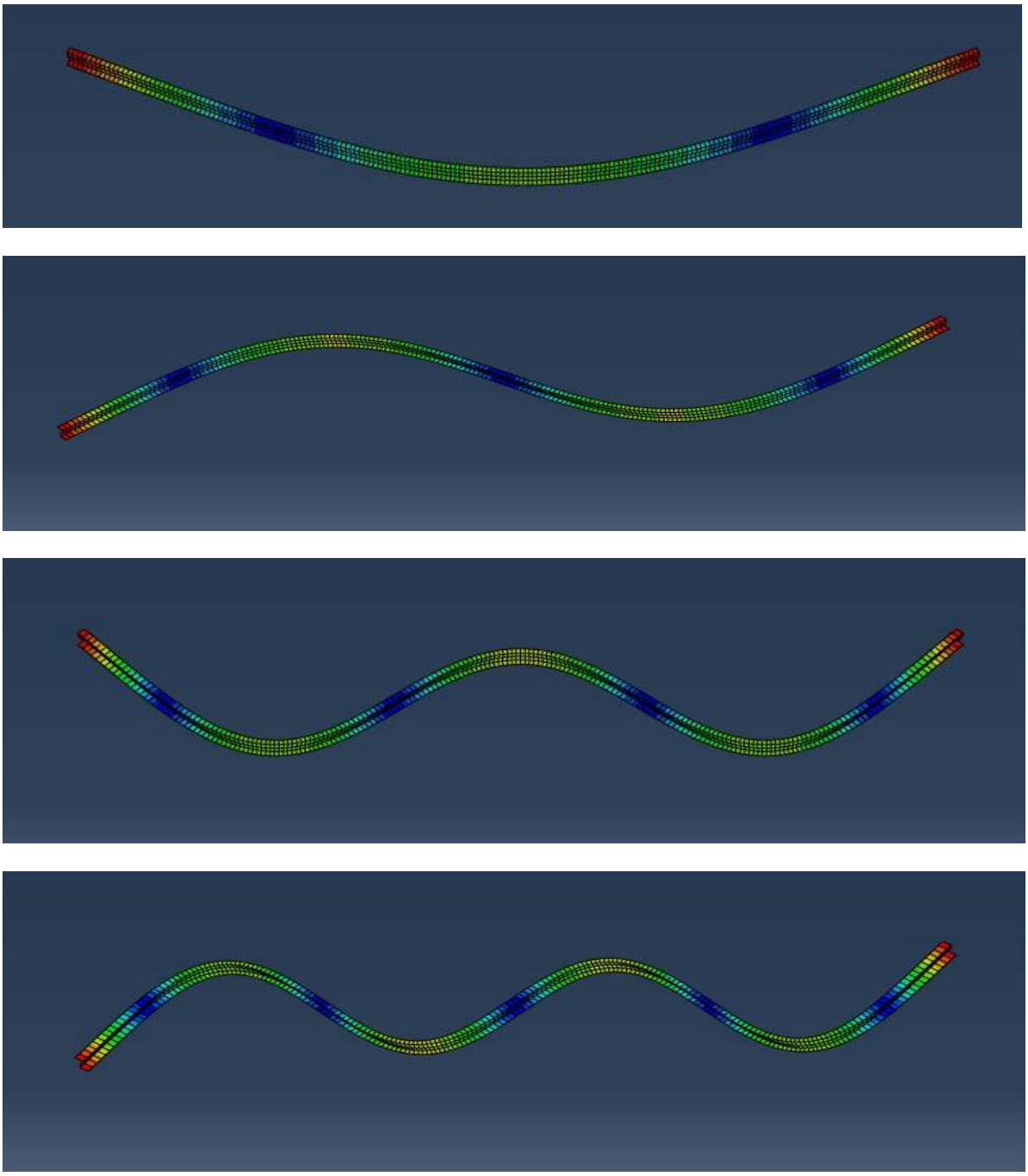

Figure 2.2.3.4.1. Four first Modal shapes of a PVB laminated glass beam

The results for the first 4 natural frequencies are compared in the table below.

Natural Frequencies computed with ABAQUS	Natural Frequencies computed with the Model
128.87 Hz	128.96 Hz
306.15 Hz	306.10 Hz
583.01 Hz	583.27 Hz
947.06 Hz	952.98 Hz

Table 2.2.3.4.1. Natural frequencies of a laminated glass beam

The values computed with ABAQUS are a little bit lower, because the plain stress elements take also the shear deformation of the glass layers into account.

3 Identification of the transverse shear modulus

For the identification of the transverse shear modulus of the polymer interlayer of the laminated glass beam, it is assumed that the isotropic elastic properties of the glass layers are known.

Young's modulus of Glass = 7.E+10 N/m2
Poisson's ratio of Glass = 0.23
Shear modulus of Glass = 2.85E+10 N/m2

It is also assumed that the Poisson's ratio of the polymer interlayer is given. For PVB, the value of Poisson's ratio v = 0.45. Assuming that the polymer material is also isotropic, the Young's modulus E can be computed from the transverse shear modulus G:

$$E = 2G(1+v)$$

The transverse shear modulus G of the polymer interlayer is hence the only unknown value. In the following paragraphs, it will be described how the value of G can be estimated from the measured first natural frequency of a freely suspended laminated glass beam.

3.1 Theory background

The background theory for the identification is given in a separate internal report. The different steps are:

- Establish starting values
- Establish smaller intervals by bisections
- Refine the values by interpolation
- Identification of the final value by iterations on the value of the transverse shear modulus based on the sensitivity of the resonance frequencies for variations of the transverse shear modulus

3.2 Example 1 of identification of G

The test beam is a laminated glass beam with a very thin PVB interlayer:

Length Beam	:	.25 m
Width Beam	:	2.93300E-02 m
Thick Glass layer	:	3.85000E-03 m
Thick Poly layer	:	3.90000E-04 m
Specific Mass Glass:		2480.0 kg/m3
Specific Mass Poly :		1100.0 kg/m3
Beam Mass	:	.14317 kg
E-modulus Glass	:	7.00000E+10 N/m2

The measured first Frequency was 698.00 Hz

The next paragraphs illustrate the starting procedure, the bisesctions, the interpolation and finally the iterations on the G value.

3.2.1 Starting value

Measured first Eigenvalue	:	1.92340E+07
Minimal Eigenvalue (independent layers)	:	4.37336E+06
Maximal Eigenvalue (monolith)	:	2.02885E+07
EI-Min	:	19.527 Nm2
EI-Max:		90.589 Nm2

Obtained starting value for the shear modulus of the PVB layer:

G_{Start} = 6.53E+10 N/m2

Young's Modulus of the PVB layer E_0 : 1.89551E+11 N/m2

3.2.2 Bisections

The first interval for the eigenvalues is bounded by the monolith and the separate beams boundaries. Next subsequent bisections isolate the measured eigenvalue between more and more sharp boundaries.

Iteration number	Transverse shear G N/m2	Computed eigenvalue	Computed natural frequency Hz	Measured natural frequency Hz
1	6.53E+010	1.99E+007	711.75	698
2	3.26E+010	1.99E+007	711.65	698
3	1.63E+010	1.99E+007	711.54	698
4	8.17E+009	1.99E+007	711.35	698
5	4.08E+009	1.99E+007	711.00	698
6	2.04E+009	1.99E+007	710.31	698
7	1.02E+009	1.98E+007	708.95	698
8	5.10E+008	1.96E+007	706.27	698
9	2.55E+008	1.94E+007	701.09	698
10	1.28E+008	1.88E+007	691.32	698

Table 3.2.2.1. G-modulus value during subsequent bisections

It can be observed that after the 10th bisection the value of the computed natural frequency became lower than the measured value. It is also observed that at the start, the value of the G modulus hardly influences the eigenvalue. This means the eigenvalue is not very sensitive for variations of G.

3.2.3 Interpolated value at the end of the bisections

At the end of the bisection the situation is as follows:

G_{Min} = 1.28E+008
G_{Max} = 2.55E+008
FREQ Min = 691.32 Hz
FREQ Max = 701.09 Hz

With these values, an interpolated value for G can be computed using (87):

$$G_{Interpolated} = 2.14E+008 \text{ N/m2}$$

3.2.4 Direct iteration on the eigenvalue expression

$$G_{Final} = 1.95E+08 \text{ N/m2}$$

FREQ Numeriek = 697.99 Hz

FREQ Measured = 698.00 Hz

The sensitivity of lambda for G = 3.73E-003

The percentage error for G for a 1 Hz Measurement error = 7.58%

This shows that a very small error on the measured frequency of 1 Hz already causes a large percentage error of 7.58%. This is due to the low sensitivity of the eigenvalue for variations of G.

3.2.5 Conclusion

Even for very lows sensitivities, the combination of bisections, interpolation and direct iteration allows estimating the transverse shear modulus of the PVB layer. However, a small error on the measured frequency immediately causes a large uncertainty on the final result for G.

3.3 Example 2 for identification of the G-Modulus

The natural frequencies computed with ABAQUS are used to validate the value of the identified shear modulus. The G-modulus is estimated with the identification procedure.

Case Nr.	$F_{Num.Model}$ [Hz]	G-Modulus Polymer [Pa]	Estimated G-Modulus [Pa]	% error on obtained shear modulus	Sensitivity of eigenvalue
1	1215	2.69E+10	2.37E+10	8.43	1.03E-05
2	1124	2.69E+09	2.69E+09	4.38	7.51E-04
3	958	2.69E+08	2.69E+09	0.73	3.85E-02
4	542	2.69E+07	2.69E+09	0.58	0.27
5	282	2.69E+06	2.69E+09	1.82	0.45
6	225	2.69E+05	2.69E+09	13.51	0.49
7	218	2.69E+04	2.66E+09	131	0.49

Table 3.3.1. Identification of the G-Modulus

The identification procedure is capable of estimating nearly all the G-Modulus values correctly. However, the given frequencies are computed hence free of error. It can be seen that the expected % error if the measured frequency is just added 1 Hz is considerable for cases 1, 2, 6 and 7. Only cases 3-5 have reasonable % errors and hence are stable.

As a test, the value of the natural frequency of case 1 and 6 is added and subtracted 1 Hz.

Case Nr.	$F_{Num.Model}$ [Hz]	G-Modulus Polymer [Pa]	Estimated G-Modulus [Pa]	% Difference for G-Modulus
1 bis	1216	2.69E+10	2.40E+10	+8.45
1 ter	1214	2.69E+09	2.33E+09	-8.4
6 bis	226	2.69E+08	3.05E+09	+11.97
6 ter	224	2.69E+07	2.32E+09	-15.53

Table 3.3.2 Error on the estimated G-Modulus by 1 Hz difference

It is instructive to plot the frequency value of the laminated beam as a function of the G-Modulus (Figure 6.6.1). A typical S-shape occurs. The two flat extremes are zones were the frequency doesn't change much with variations of the G-

Modulus. The flat parts are zones of low sensitivity hence not suitable for identification of the G-modulus.

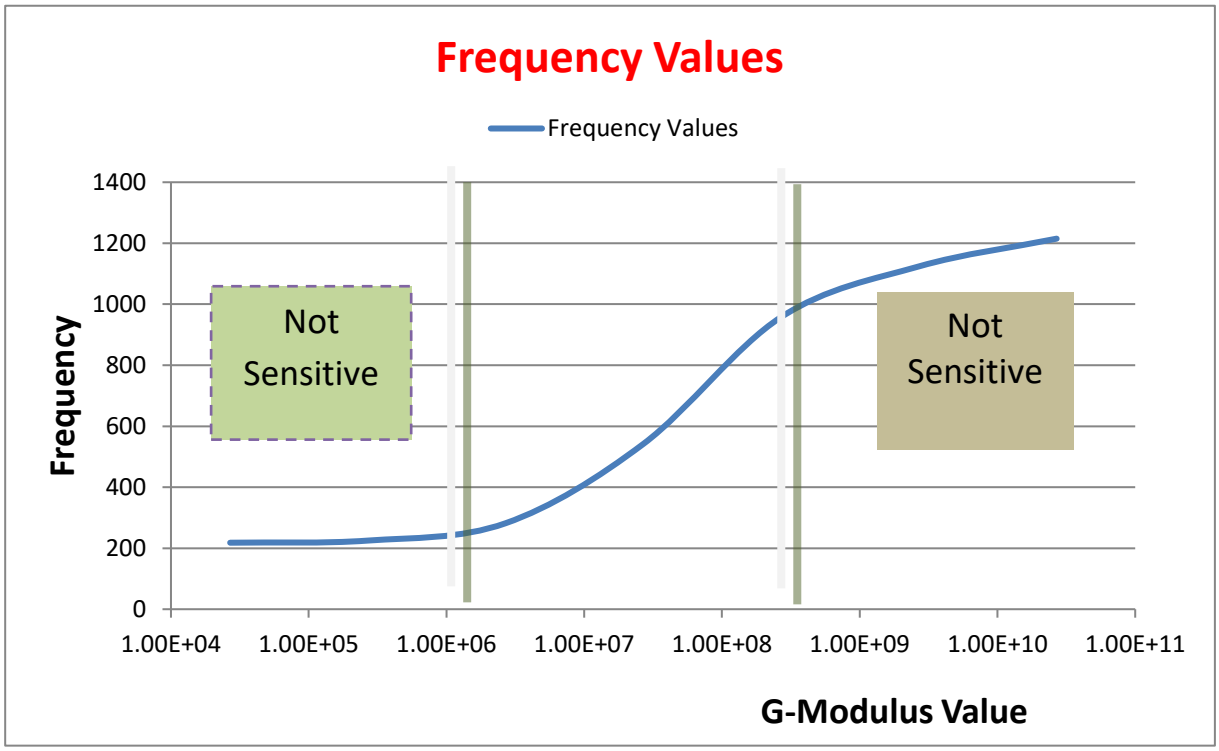

Figure 3.3.1. Evolution of the frequency as a function of the G-Modulus value

3.4 Validation of identification by data from literature

Identification based on data given in references:

[1] Barbora H´alkov´a. Experimental and numerical modelling of PVB foil. Master's thesis, Czech Technical University In Prague, 2024.

[2] Alena Zemanov´a, Jan Zeman, Tom´aˇs Janda, Jaroslav Schmidt, and Michal ˇ Sejnoha. On modal analysis of laminated glass: Usability of simplified methods and enhanced effective thickness. Composites Part B: Engineering, 151:92–105, 2018

Input values

Thickness glass layers:	4.93 mm
Thickness PVB layer:	1.28 mm
Width test beam:	0.03 m
E-Modulus glass:	71 GPa
Poisson ratio glass:	0.23
Density glass:	2473 kg/m3
Density PVB:	1100 kg/m3

Name	Length [m]	Measured frequency [Hz]	Measured damping ratio [%]	G-modul. Refer. [MPa]	G-Modul. Identific. [MPa]	Tangents Refer. [%]	Tangents Identific. [%]
DSR-PVB	0.300	585.6	1.515	47.89	47.84	11.49	11.5
	0.250	803.2	2.075	49.20	49.24	13.45	13.5
	0.200	1173.4	2.670	51.55	51.60	14.95	15.2
	0.150	1892.7	2.810	55.22	55.11	14.24	14.5
DSR-LG	0.300	692.4	0.54	843.11	889.4	46.44	40.6
	0.250	991.5	0.7	922.93	964.1	46.87	40.4
	0.200	1535.1	0.935	1045.48	1073	46.68	39.8
	0.150	2680.7	1.32	1215.77	1210	45.52	38.0
Mixed	0.300	672.5	1.355	249.83	267.8	35.83	34.4
	0.250	953.9	1.36	275.53	282.8	27.87	26.7
	0.200	1451.3	1.3	295.71	292.7	19.46	18.7
	0.150	2452.0	1.15	308.0	298.6	11.88	11.4

Table 3.4.1. Evolution of the frequency as a function of the G-Modulus value

"DSR-LG" and "Mixed" have very stif PVB layers, hence the laminate behavior is close to classic laminate behaviour (no influence of transverse shear deformations). This makes the sensitivity of the frequencies for changes of G-value very low (see example the not sensitive area at the right side of figure 3.3.1). A thicker PVB layer would help increasing the sensitivity.

"DSR-PVB" has a much higher sensitivity (middle area of figure 3.3.1); hence the identification results are more reliable.

4 Manual for FTN Sandwich beam programs

The Fortran programs for sandwich analysis have several versions:

- **Sandwich_eig.exe**: computation of the resonance frequencies, modal shapes, Bending moment and shear force distribution, potential and kinetic energy. The output is connected to a visual studio program "**Sandwich_design**" that enables the graphical representation of the results
- **Sandwich_3P.exe**: computation of the deformation due to 3-point bending. Additionally, the Bending moment and shear force distribution, are computed. The output is connected to a visual studio program "**Sandwich_design**" that enables the graphical representation of the results
- **Sandwich_4P.exe**: computation of the deformation due to 4-point bending. Additionally, the Bending moment and shear force distribution, are computed. The output is connected to a visual studio program "**Sandwich_design**" that enables the graphical representation of the results

There are also 2 Fortran programs for identification of the transverse shear modulus, based on measured resonance frequencies and damping ratios.

- **Sandwich_Resonalyser.exe**: identification of transverse shear modulus for sandwich beams with constant inner layer. Output provides sensitivities of the frequency for transverse shear variations, apparent beam stiffness and potential energy of skins and inner layers and kinetic energy. The visual studio program "**Beam_Properties**" provides graphical output.
- **Sandwich_VarThick.exe**: same as previous, but allows additionally variable thickness of the inner layer. The visual studio program "**Beam_Properties**" provides graphical output.

4.1 Sandwich_eig: resonance frequencies of a sandwich beam

FTN Program Sandwich_Eig.exe can compute up to 10 resonance frequencies and associated mode shapes of a sandwich beam.

4.1.1 Input File: c:\Ident_net\Geom_Files\Input_Eig.txt

read(2,*)BLENGTH	Length of the beam [m]
read(2,*)BWIDTH	Width of the beam [m]
read(2,*)H	Skin thickness [m]
read(2,*)H0	Core thickness [m]
read(2,*)RHO	Skin density [kg/m3],
read(2,*)RHO0	Core density [kg/m3]
read(2,*)EGLAS	Young ‘s Modulus skin [kg/m3]
read(2,*)EPOLY	Young ‘s Modulus core [kg/m3]
read(2,*)GPOLY	Transverse shear modulus core [Pa]
read(2,*)NMEIG	Number of desired frequencies
read(2,*)FREQMI	Value of min frequency boundary
read(2,*)FREQMA	Value of max frequency boundary
read(2,*)KODAC	Accelerometer node position
read(2,*)ACCELM	Accelerometer mass

Example input File

```
0.3000000
0.0302000
0.0049430
0.0022400
2.475E+03
1.065E+03
7.0900E+10
4.231E+08
 1.511E+08
1
1
1000
5
0.0
```

4.1.2 Output File: c:\Ident_net\Geom_Files\Output_Eig.txt

```
&&& BEAM PROPERTIES :

 Length Beam       :            .30000
 Width  Beam       :          3.02000E-02
 Thick Skin layer  :          4.94300E-03
 Thick Poly layer  :          2.24000E-03
 Specific Mass Skin:            2475.0
 Specific Mass Poly :           1065.0
 Beam Mass         :           .24329
 E-modulus Skin    :           7.09000E+10
 E-modulus Poly    :           4.23100E+08
 G-modulus Poly    :           1.51100E+08
 Accelerometer node:            5
 Accelerometer Mass :             .00000
```

```
   &&&  EIGENVALUE SPECIFICATIONS


        NUMBER OF EIGENFREQUENCIES    :      1
        LOWER LIMIT EIGENFREQUENCIES  :      1.0000
        HIGHER LIMIT EIGENFREQUENCIES :      1000.0


 RESULTS OF THE CALCULATIONS
 ---------------------------

   ******************************************
   *  NO  *       EIGENFREQUENCY       * BIS. * ITER.*
   ******************************************
   *   1  *    689.070168627662       *  1  *  25     *
   ******************************************


   &&& SECTION FORCE OUTPUT FIRST MODE

     SHEAR FORCE       BENDING MOMENT

    1    .00000           .00000
    2  -2.77802E+06        -45486.
    3  -3.99377E+06       -1.51008E+05
    4  -3.69693E+06       -2.69898E+05
    5  -2.18670E+06       -3.60608E+05
    6    150.31            -3.94286E+05
    7   2.18700E+06       -3.60599E+05
    8   3.69723E+06       -2.69880E+05
    9   3.99407E+06       -1.50981E+05
   10   2.77832E+06        -45450.
   11    .00000             .00000


The sensitivity of lambda for G =   2.474548073677854E-002
The sensitivity of lambda for E =   2.116370387283636E-004


COMPUTATION OF THE MAXIMAL POSSIBLE SANDWICH FREQUENCY

        APPARENT BEAM STIFFNESS VALUE:          245.78
        MAXIMAL CLT BEAM STIFFNESS:             316.15
        SANDWICH STIFFNESS PER METER:           8138.3
        MAXIMAL SANDWICH STIFFNESS PER METER:     10469.

        COMPUTED SANDWICH FREQUENCY:          689.07

        TOTAL POTENTIAL ENERGY:              9.37253E+06
        CONTRIBUTION BENDING MOMENT:         1.69830E+06
        CONTRIBUTION NORMAL FORCE:           5.80424E+06
        CONTRIBUTION SHEAR FORCE:            1.86952E+06
        CONTRIBUTION BENDING CORE:            471.58


        TOTAL KINETIC ENERGY:                9.37253E+06
        CONTRIBUTION MASS:                   9.32301E+06
        CONTRIBUTION INERTIA:                49519.
```

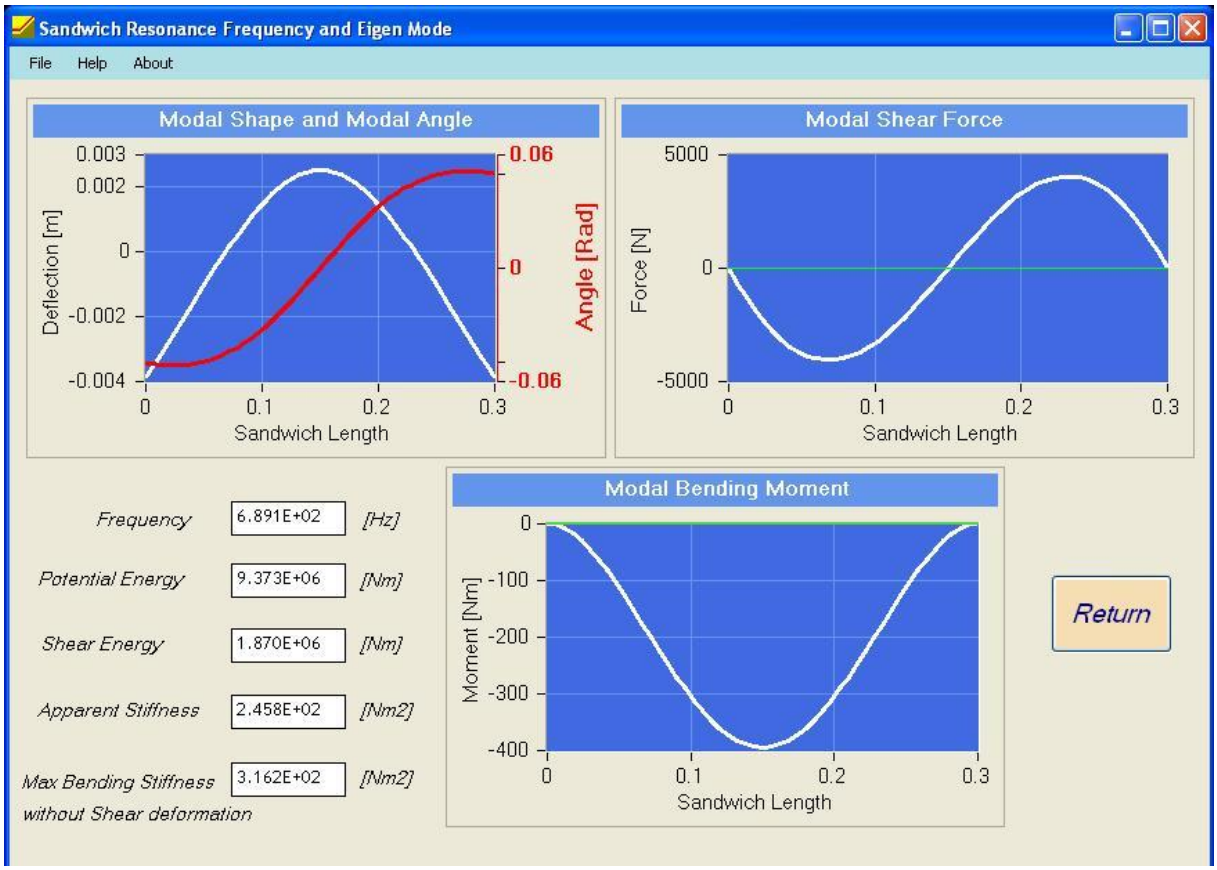

Figure 4.1.2.1 Graphical representation results of vibration analysis

4.2 3-point bending of a sandwich beam

FTN Program Sandwich_3P.exe computes the deformation and stresses and moments due to a concentrated load in the middle of the beam. The extreme end of the beam are simply supported (3-Point bending configuration)

4.2.1 Input File: c:\Ident_net\Geom_Files\Input_3P.txt

read(2,*)BLENGTH	Length of the beam [m]
read(2,*)BWIDTH	Width of the beam [m]
read(2,*)H	Skin thickness [m]
read(2,*)H0	Core thickness [m]
read(2,*)RHO	Skin density [kg/m3],
read(2,*)RHO0	Core density [kg/m3]
read(2,*)EGLAS	Young ‘s Modulus skin [kg/m3]
read(2,*)EPOLY	Young ‘s Modulus core [kg/m3]
read(2,*)GPOLY	Transverse shear modulus [Pa]
read(2,*)QLOAD	Concentrated load in the middle [N]

Example input File

0.3000000
0.0302000
0.0049430
0.0022400
2.475E+03
1.065E+03
7.0900E+10
4.231E+08
1.511E+08
1.000E+02

4.2.2 Output File: c:\Ident_net\Geom_Files\Output_3P.txt

Example:

```
*****************************************************************************
*                                       *
*              STATIC ANALYSIS PROGRAM                  *
*                                       *
*****************************************************************************


     &&&  CONTROL INFORMATION

          NUMBER OF NODAL POINTS   :        11
          POINT LOAD IN BEAM MIDDLE :          100.00


     &&& BEAM PROPERTIES :


          Length Beam     :               .30000
          Width  Beam     :              3.02000E-02
          thick skin layer :             4.94300E-03
          thick core layer :             2.24000E-03
          E-modulus Skin   :              7.09000E+10
          E-modulus Core   :              4.23100E+08
          G-modulus Core   :              1.51100E+08
          Transvere Load   :              100.00



*****************************************************************************
*                                       *
*              RESULTS                        *
*                                       *
*****************************************************************************



     node     .displacement  rotation

      1    .0000E+00   -.1891E-02
      2    .6339E-04   -.1823E-02
      3    .1222E-03   -.1598E-02
      4    .1725E-03   -.1256E-02
      5    .2096E-03   -.7228E-03
      6    .2238E-03   -.2752E-12
      7    .2096E-03    .7228E-03
      8    .1725E-03    .1256E-02
      9    .1222E-03    .1598E-02
     10    .6339E-04    .1823E-02
     11    .0000E+00    .1891E-02

Reaction Force 1 =     -50.000000033288560
Reaction Force 2 =     -49.999999960493820
```

DEFLECTIONS

	COORDINATE	DEFLECTION
1	.000E+00	.000E+00
2	.600E-02	.128E-04
3	.120E-01	.255E-04
4	.180E-01	.382E-04
5	.240E-01	.509E-04
6	.300E-01	.634E-04
7	.360E-01	.757E-04
8	.420E-01	.878E-04
9	.480E-01	.996E-04
10	.540E-01	.111E-03
11	.600E-01	.122E-03
12	.660E-01	.133E-03
13	.720E-01	.143E-03
14	.780E-01	.154E-03
15	.840E-01	.163E-03
16	.900E-01	.173E-03
17	.960E-01	.181E-03
18	.102E+00	.189E-03
19	.108E+00	.197E-03
20	.114E+00	.204E-03
21	.120E+00	.210E-03
22	.126E+00	.215E-03
23	.132E+00	.219E-03
24	.138E+00	.221E-03
25	.144E+00	.223E-03
26	.150E+00	.224E-03
27	.156E+00	.223E-03
28	.162E+00	.221E-03
29	.168E+00	.219E-03
30	.174E+00	.215E-03
31	.180E+00	.210E-03
32	.186E+00	.204E-03
33	.192E+00	.197E-03
34	.198E+00	.189E-03
35	.204E+00	.181E-03
36	.210E+00	.173E-03
37	.216E+00	.163E-03
38	.222E+00	.154E-03
39	.228E+00	.143E-03
40	.234E+00	.133E-03
41	.240E+00	.122E-03
42	.246E+00	.111E-03
43	.252E+00	.996E-04
44	.258E+00	.878E-04
45	.264E+00	.757E-04
46	.270E+00	.634E-04
47	.276E+00	.509E-04
48	.282E+00	.382E-04
49	.288E+00	.255E-04
50	.294E+00	.128E-04
51	.300E+00	.000E+00

GLOBAL ANGLES

	COORDINATE	ALFA	THETA	GAMMA	PHIE
1	.000E+00	-.189E-02	-.213E-02	.132E-02	-.817E-03
2	.600E-02	-.188E-02	-.212E-02	.129E-02	-.830E-03
3	.120E-01	-.188E-02	-.212E-02	.131E-02	-.808E-03
4	.180E-01	-.187E-02	-.212E-02	.134E-02	-.776E-03
5	.240E-01	-.185E-02	-.210E-02	.135E-02	-.749E-03
6	.300E-01	-.182E-02	-.207E-02	.135E-02	-.727E-03
7	.360E-01	-.179E-02	-.203E-02	.133E-02	-.708E-03
8	.420E-01	-.175E-02	-.199E-02	.130E-02	-.688E-03
9	.480E-01	-.170E-02	-.194E-02	.128E-02	-.661E-03
10	.540E-01	-.165E-02	-.189E-02	.126E-02	-.624E-03
11	.600E-01	-.160E-02	-.183E-02	.126E-02	-.573E-03
12	.660E-01	-.154E-02	-.177E-02	.126E-02	-.509E-03

13	.720E-01	-.148E-02	-.171E-02	.128E-02	-.433E-03
14	.780E-01	-.141E-02	-.165E-02	.130E-02	-.348E-03
15	.840E-01	-.134E-02	-.158E-02	.132E-02	-.260E-03
16	.900E-01	-.126E-02	-.150E-02	.133E-02	-.172E-03
17	.960E-01	-.117E-02	-.141E-02	.132E-02	-.899E-04
18	.102E+00	-.107E-02	-.131E-02	.129E-02	-.181E-04
19	.108E+00	-.964E-03	-.119E-02	.123E-02	.395E-04
20	.114E+00	-.848E-03	-.106E-02	.114E-02	.805E-04
21	.120E+00	-.723E-03	-.910E-03	.101E-02	.103E-03
22	.126E+00	-.590E-03	-.748E-03	.856E-03	.109E-03
23	.132E+00	-.449E-03	-.573E-03	.670E-03	.975E-04
24	.138E+00	-.303E-03	-.388E-03	.461E-03	.730E-04
25	.144E+00	-.152E-03	-.196E-03	.235E-03	.390E-04
26	.150E+00	-.275E-12	-.421E-12	.789E-12	.368E-12
27	.156E+00	.152E-03	.196E-03	-.235E-03	-.390E-04
28	.162E+00	.303E-03	.388E-03	-.461E-03	-.730E-04
29	.168E+00	.449E-03	.573E-03	-.670E-03	-.975E-04
30	.174E+00	.590E-03	.748E-03	-.856E-03	-.109E-03
31	.180E+00	.723E-03	.910E-03	-.101E-02	-.103E-03
32	.186E+00	.848E-03	.106E-02	-.114E-02	-.805E-04
33	.192E+00	.964E-03	.119E-02	-.123E-02	-.395E-04
34	.198E+00	.107E-02	.131E-02	-.129E-02	.181E-04
35	.204E+00	.117E-02	.141E-02	-.132E-02	.899E-04
36	.210E+00	.126E-02	.150E-02	-.133E-02	.172E-03
37	.216E+00	.134E-02	.158E-02	-.132E-02	.260E-03
38	.222E+00	.141E-02	.165E-02	-.130E-02	.348E-03
39	.228E+00	.148E-02	.171E-02	-.128E-02	.433E-03
40	.234E+00	.154E-02	.177E-02	-.126E-02	.509E-03
41	.240E+00	.160E-02	.183E-02	-.126E-02	.573E-03
42	.246E+00	.165E-02	.189E-02	-.126E-02	.624E-03
43	.252E+00	.170E-02	.194E-02	-.128E-02	.661E-03
44	.258E+00	.175E-02	.199E-02	-.130E-02	.688E-03
45	.264E+00	.179E-02	.203E-02	-.133E-02	.708E-03
46	.270E+00	.182E-02	.207E-02	-.135E-02	.727E-03
47	.276E+00	.185E-02	.210E-02	-.135E-02	.749E-03
48	.282E+00	.187E-02	.212E-02	-.134E-02	.776E-03
49	.288E+00	.188E-02	.212E-02	-.131E-02	.808E-03
50	.294E+00	.188E-02	.212E-02	-.129E-02	.830E-03
51	.300E+00	.189E-02	.213E-02	-.132E-02	.817E-03

TOTAL FORCE AND MOMENTS IN THE SANDWICH

	COORDINATE	NORMAL	T-MOMENT	M-SKIN	M-NORMAL	M-CORE
1	.000E+00	.664E+01	-.205E+00	-.787E-01	-.477E-01	-.437E-04
2	.600E-02	.339E+02	-.264E+00	-.105E-01	-.243E+00	-.582E-05
3	.120E-01	.687E+02	-.510E+00	-.810E-02	-.494E+00	-.450E-05
4	.180E-01	.107E+03	-.844E+00	-.384E-01	-.767E+00	-.213E-04
5	.240E-01	.146E+03	-.120E+01	-.797E-01	-.105E+01	-.443E-04
6	.300E-01	.183E+03	-.156E+01	-.119E+00	-.132E+01	-.663E-04
7	.360E-01	.220E+03	-.188E+01	-.151E+00	-.158E+01	-.839E-04
8	.420E-01	.255E+03	-.218E+01	-.173E+00	-.183E+01	-.962E-04
9	.480E-01	.289E+03	-.245E+01	-.187E+00	-.208E+01	-.104E-03
10	.540E-01	.323E+03	-.271E+01	-.194E+00	-.232E+01	-.108E-03
11	.600E-01	.357E+03	-.296E+01	-.200E+00	-.256E+01	-.111E-03
12	.660E-01	.391E+03	-.322E+01	-.208E+00	-.281E+01	-.115E-03
13	.720E-01	.426E+03	-.350E+01	-.220E+00	-.306E+01	-.122E-03
14	.780E-01	.462E+03	-.380E+01	-.239E+00	-.332E+01	-.133E-03
15	.840E-01	.499E+03	-.412E+01	-.266E+00	-.358E+01	-.148E-03
16	.900E-01	.536E+03	-.445E+01	-.302E+00	-.385E+01	-.168E-03
17	.960E-01	.573E+03	-.481E+01	-.346E+00	-.412E+01	-.192E-03
18	.102E+00	.609E+03	-.517E+01	-.396E+00	-.438E+01	-.220E-03
19	.108E+00	.644E+03	-.552E+01	-.450E+00	-.462E+01	-.250E-03
20	.114E+00	.676E+03	-.587E+01	-.505E+00	-.486E+01	-.280E-03
21	.120E+00	.705E+03	-.618E+01	-.558E+00	-.506E+01	-.310E-03
22	.126E+00	.730E+03	-.646E+01	-.607E+00	-.524E+01	-.337E-03
23	.132E+00	.750E+03	-.669E+01	-.648E+00	-.539E+01	-.360E-03
24	.138E+00	.765E+03	-.686E+01	-.679E+00	-.550E+01	-.377E-03
25	.144E+00	.774E+03	-.696E+01	-.699E+00	-.556E+01	-.388E-03
26	.150E+00	.777E+03	-.700E+01	-.705E+00	-.558E+01	-.392E-03
27	.156E+00	.774E+03	-.696E+01	-.699E+00	-.556E+01	-.388E-03

28	.162E+00	.765E+03	-.686E+01	-.679E+00	-.550E+01	-.377E-03
29	.168E+00	.750E+03	-.669E+01	-.648E+00	-.539E+01	-.360E-03
30	.174E+00	.730E+03	-.646E+01	-.607E+00	-.524E+01	-.337E-03
31	.180E+00	.705E+03	-.618E+01	-.558E+00	-.506E+01	-.310E-03
32	.186E+00	.676E+03	-.587E+01	-.505E+00	-.486E+01	-.280E-03
33	.192E+00	.644E+03	-.552E+01	-.450E+00	-.462E+01	-.250E-03
34	.198E+00	.609E+03	-.517E+01	-.396E+00	-.438E+01	-.220E-03
35	.204E+00	.573E+03	-.481E+01	-.346E+00	-.412E+01	-.192E-03
36	.210E+00	.536E+03	-.445E+01	-.302E+00	-.385E+01	-.168E-03
37	.216E+00	.499E+03	-.412E+01	-.266E+00	-.358E+01	-.148E-03
38	.222E+00	.462E+03	-.380E+01	-.239E+00	-.332E+01	-.133E-03
39	.228E+00	.426E+03	-.350E+01	-.220E+00	-.306E+01	-.122E-03
40	.234E+00	.391E+03	-.322E+01	-.208E+00	-.281E+01	-.115E-03
41	.240E+00	.357E+03	-.296E+01	-.200E+00	-.256E+01	-.111E-03
42	.246E+00	.323E+03	-.271E+01	-.194E+00	-.232E+01	-.108E-03
43	.252E+00	.289E+03	-.245E+01	-.187E+00	-.208E+01	-.104E-03
44	.258E+00	.255E+03	-.218E+01	-.173E+00	-.183E+01	-.962E-04
45	.264E+00	.220E+03	-.188E+01	-.151E+00	-.158E+01	-.839E-04
46	.270E+00	.183E+03	-.156E+01	-.119E+00	-.132E+01	-.663E-04
47	.276E+00	.146E+03	-.120E+01	-.797E-01	-.105E+01	-.443E-04
48	.282E+00	.107E+03	-.844E+00	-.384E-01	-.767E+00	-.213E-04
49	.288E+00	.687E+02	-.510E+00	-.810E-02	-.494E+00	-.450E-05
50	.294E+00	.339E+02	-.264E+00	-.105E-01	-.243E+00	-.582E-05
51	.300E+00	.664E+01	-.205E+00	-.787E-01	-.477E-01	-.437E-04

MAXIMAL STRESS VALUE IN SKIN = 1.094318185084931E+007
EQUIVALENT EI SANDWICH BEAM= 213.727012925228600

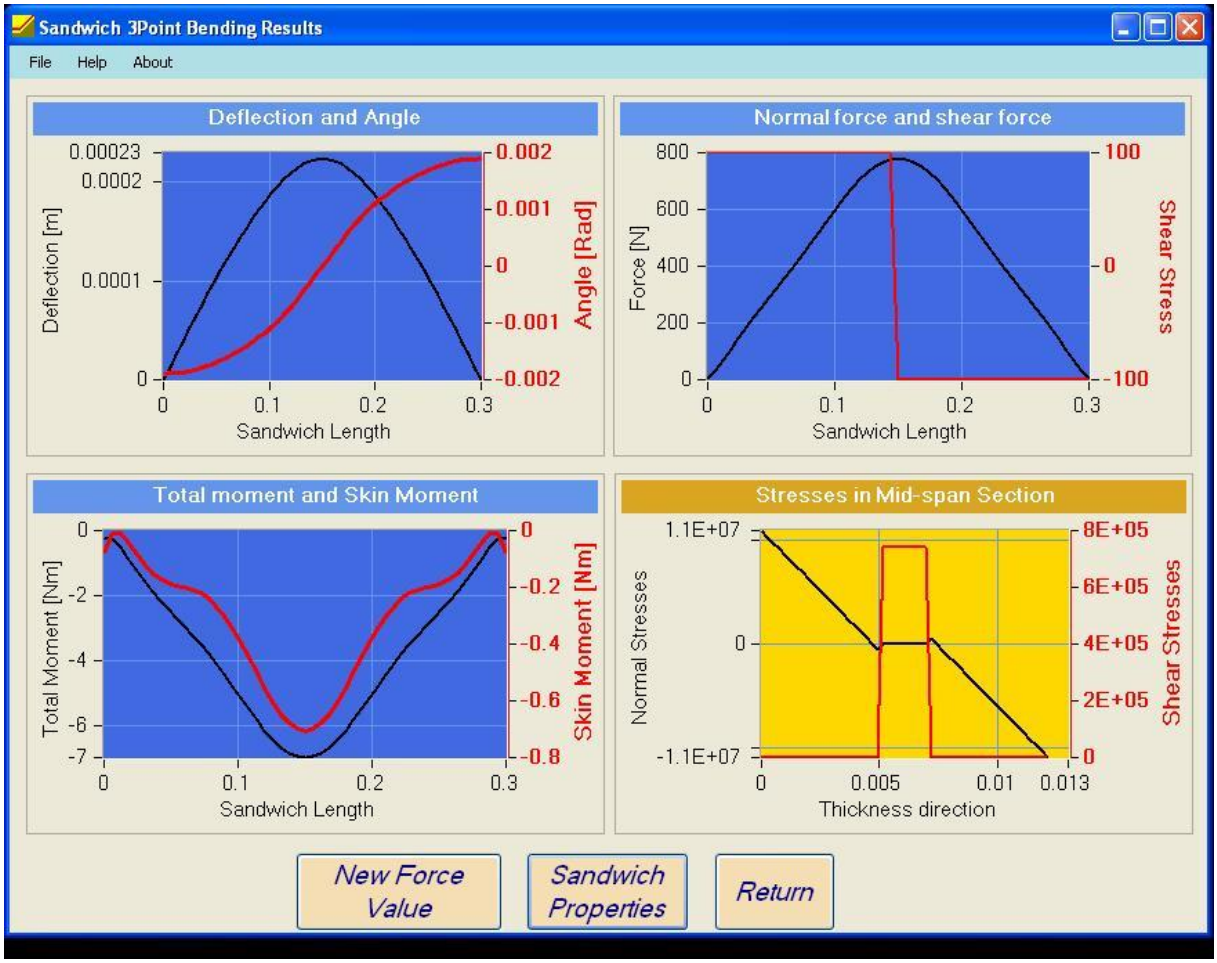

Figure 4.2.2.1 Graphical representation results 3-Point bending

4.2.3 Output File: c:\Ident_net\Geom_Files\Output_3P.CSV

All the results of the computations are also stored in a CSV File for further processing using the MS program EXCELL.

4.3 4-point bending of a sandwich beam

FTN Program Sandwich_4P.exe computes the deformation and stresses and moments due to two symmetrical concentrated loads on each side of the beam. The beam is simply supported in two symmetrical positions (4-Point bending configuration) at a distance of the load positions.

4.3.1 Input File: c:\Ident_net\Geom_Files\Input_4P.txt

read(2,*)BLENGTH	Length of the beam [m]
read(2,*)BWIDTH	Width of the beam [m]
read(2,*)H	Skin thickness [m]
read(2,*)H0	Core thickness [m]
read(2,*)RHO	Skin density [kg/m3],
read(2,*)RHO0	Core density [kg/m3]
read(2,*)EGLAS	Young ‘s Modulus skin [kg/m3]
read(2,*)EPOLY	Young ‘s Modulus core [kg/m3]
read(2,*)GPOLY	Transverse shear modulus [Pa]
read(2,*)QLOAD	Value of the 2-point load in the middle [N]
read(1,*)DIST	Distance to the 2 load points [m]

Example input File

```
0.3000000
0.0302000
0.0049430
0.0022400
2.475E+03
1.065E+03
7.0900E+10
4.231E+08
 1.511E+08
1.000E+02
 .05
```

4.3.2 Output File: c:\Ident_net\Geom_Files\Output_4P.text

```
*****************************************************************************
*                                       *
*              STATIC ANALYSIS PROGRAM                  *
*                                       *
*****************************************************************************


     &&&  CONTROL INFORMATION

          NUMBER OF NODAL POINTS   :        11
          VALUE OF THE 2 POINT LOADS:          100.00
          DISTANCE TO 2 LOAD POINTS :         5.00000E-02


     &&& BEAM PROPERTIES :


          Length Beam     :               .30000
          Width  Beam     :              3.02000E-02
          thick skin layer :             4.94300E-03
          thick core layer :             2.24000E-03
          E-modulus Skin   :              7.09000E+10
          E-modulus Core   :              4.23100E+08
          G-modulus Core   :              1.51100E+08
          Transvere Load   :              100.00



     node     .displacement  rotation

       1    .0000E+00   -.9014E-03
       2    .3173E-04   -.8047E-03
       3    .5582E-04   -.5942E-03
       4    .7128E-04   -.3842E-03
       5    .8006E-04   -.1914E-03
       6    .8299E-04   -.1119E-12
       7    .8006E-04    .1914E-03
       8    .7128E-04    .3842E-03
       9    .5582E-04    .5942E-03
      10    .3173E-04    .8047E-03
      11    .0000E+00    .9014E-03

Reaction Force 1 =     -50.000000013430670
Reaction Force 2 =     -49.999999983994940


DEFLECTIONS

  COORDINATE    DEFLECTION

  1 .000E+00  .000E+00
  2 .600E-02  .665E-05
  3 .120E-01  .132E-04
  4 .180E-01  .197E-04
  5 .240E-01  .258E-04
  6 .300E-01  .317E-04
  7 .360E-01  .373E-04
  8 .420E-01  .425E-04
  9 .480E-01  .473E-04
 10 .540E-01  .517E-04
 11 .600E-01  .558E-04
 12 .660E-01  .595E-04
 13 .720E-01  .629E-04
 14 .780E-01  .660E-04
 15 .840E-01  .688E-04
```

16	.900E-01	.713E-04
17	.960E-01	.735E-04
18	.102E+00	.755E-04
19	.108E+00	.773E-04
20	.114E+00	.788E-04
21	.120E+00	.801E-04
22	.126E+00	.811E-04
23	.132E+00	.819E-04
24	.138E+00	.825E-04
25	.144E+00	.829E-04
26	.150E+00	.830E-04
27	.156E+00	.829E-04
28	.162E+00	.825E-04
29	.168E+00	.819E-04
30	.174E+00	.811E-04
31	.180E+00	.801E-04
32	.186E+00	.788E-04
33	.192E+00	.773E-04
34	.198E+00	.755E-04
35	.204E+00	.735E-04
36	.210E+00	.713E-04
37	.216E+00	.688E-04
38	.222E+00	.660E-04
39	.228E+00	.629E-04
40	.234E+00	.595E-04
41	.240E+00	.558E-04
42	.246E+00	.517E-04
43	.252E+00	.473E-04
44	.258E+00	.425E-04
45	.264E+00	.373E-04
46	.270E+00	.317E-04
47	.276E+00	.258E-04
48	.282E+00	.197E-04
49	.288E+00	.132E-04
50	.294E+00	.665E-05
51	.300E+00	.000E+00

GLOBAL ANGLES

COORDINATE	ALFA	THETA	GAMMA	PHIE
1	.000E+00	-.901E-03	-.111E-02	.112E-02	.124E-04
2	.600E-02	-.898E-03	-.110E-02	.112E-02	.125E-04
3	.120E-01	-.886E-03	-.109E-02	.108E-02	-.658E-05
4	.180E-01	-.866E-03	-.105E-02	.101E-02	-.413E-04
5	.240E-01	-.838E-03	-.101E-02	.921E-03	-.871E-04
6	.300E-01	-.805E-03	-.955E-03	.816E-03	-.139E-03
7	.360E-01	-.767E-03	-.897E-03	.704E-03	-.192E-03
8	.420E-01	-.725E-03	-.835E-03	.591E-03	-.243E-03
9	.480E-01	-.682E-03	-.772E-03	.484E-03	-.288E-03
10	.540E-01	-.638E-03	-.709E-03	.385E-03	-.325E-03
11	.600E-01	-.594E-03	-.649E-03	.298E-03	-.351E-03
12	.660E-01	-.550E-03	-.592E-03	.224E-03	-.368E-03
13	.720E-01	-.507E-03	-.538E-03	.164E-03	-.374E-03
14	.780E-01	-.465E-03	-.487E-03	.117E-03	-.370E-03
15	.840E-01	-.424E-03	-.439E-03	.820E-04	-.358E-03
16	.900E-01	-.384E-03	-.395E-03	.570E-04	-.338E-03
17	.960E-01	-.345E-03	-.352E-03	.402E-04	-.312E-03
18	.102E+00	-.306E-03	-.311E-03	.295E-04	-.282E-03
19	.108E+00	-.268E-03	-.272E-03	.231E-04	-.249E-03
20	.114E+00	-.229E-03	-.233E-03	.192E-04	-.214E-03
21	.120E+00	-.191E-03	-.194E-03	.165E-04	-.178E-03
22	.126E+00	-.153E-03	-.156E-03	.142E-04	-.142E-03
23	.132E+00	-.115E-03	-.117E-03	.114E-04	-.106E-03
24	.138E+00	-.768E-04	-.783E-04	.813E-05	-.702E-04
25	.144E+00	-.384E-04	-.392E-04	.423E-05	-.350E-04
26	.150E+00	-.112E-12	-.171E-12	.320E-12	.149E-12
27	.156E+00	.384E-04	.392E-04	-.423E-05	.350E-04
28	.162E+00	.768E-04	.783E-04	-.813E-05	.702E-04
29	.168E+00	.115E-03	.117E-03	-.114E-04	.106E-03
30	.174E+00	.153E-03	.156E-03	-.142E-04	.142E-03

31	.180E+00	.191E-03	.194E-03	-.165E-04	.178E-03
32	.186E+00	.229E-03	.233E-03	-.192E-04	.214E-03
33	.192E+00	.268E-03	.272E-03	-.231E-04	.249E-03
34	.198E+00	.306E-03	.311E-03	-.295E-04	.282E-03
35	.204E+00	.345E-03	.352E-03	-.402E-04	.312E-03
36	.210E+00	.384E-03	.395E-03	-.570E-04	.338E-03
37	.216E+00	.424E-03	.439E-03	-.820E-04	.358E-03
38	.222E+00	.465E-03	.487E-03	-.117E-03	.370E-03
39	.228E+00	.507E-03	.538E-03	-.164E-03	.374E-03
40	.234E+00	.550E-03	.592E-03	-.224E-03	.368E-03
41	.240E+00	.594E-03	.649E-03	-.298E-03	.351E-03
42	.246E+00	.638E-03	.709E-03	-.385E-03	.325E-03
43	.252E+00	.682E-03	.772E-03	-.484E-03	.288E-03
44	.258E+00	.725E-03	.835E-03	-.591E-03	.243E-03
45	.264E+00	.767E-03	.897E-03	-.704E-03	.192E-03
46	.270E+00	.805E-03	.955E-03	-.816E-03	.139E-03
47	.276E+00	.838E-03	.101E-02	-.921E-03	.871E-04
48	.282E+00	.866E-03	.105E-02	-.101E-02	.413E-04
49	.288E+00	.886E-03	.109E-02	-.108E-02	.658E-05
50	.294E+00	.898E-03	.110E-02	-.112E-02	-.125E-04
51	.300E+00	.901E-03	.111E-02	-.112E-02	-.124E-04

TOTAL MOMENTS IN THE SANDWICH

	COORDINATE	T-MOMENT	M-SKIN	M-NORMAL	M-CORE
1	.000E+00	.235E-01	.160E-01	-.863E-02	.891E-05
2	.600E-02	-.301E+00	-.412E-01	-.218E+00	-.229E-04
3	.120E-01	-.624E+00	-.947E-01	-.434E+00	-.526E-04
4	.180E-01	-.923E+00	-.141E+00	-.642E+00	-.781E-04
5	.240E-01	-.119E+01	-.177E+00	-.835E+00	-.981E-04
6	.300E-01	-.141E+01	-.202E+00	-.101E+01	-.112E-03
7	.360E-01	-.159E+01	-.218E+00	-.116E+01	-.121E-03
8	.420E-01	-.173E+01	-.226E+00	-.128E+01	-.125E-03
9	.480E-01	-.184E+01	-.226E+00	-.139E+01	-.125E-03
10	.540E-01	-.191E+01	-.221E+00	-.147E+01	-.122E-03
11	.600E-01	-.196E+01	-.211E+00	-.154E+01	-.117E-03
12	.660E-01	-.199E+01	-.200E+00	-.159E+01	-.111E-03
13	.720E-01	-.200E+01	-.188E+00	-.163E+01	-.104E-03
14	.780E-01	-.201E+01	-.176E+00	-.165E+01	-.979E-04
15	.840E-01	-.201E+01	-.166E+00	-.168E+01	-.919E-04
16	.900E-01	-.200E+01	-.156E+00	-.169E+01	-.868E-04
17	.960E-01	-.200E+01	-.149E+00	-.170E+01	-.829E-04
18	.102E+00	-.200E+01	-.144E+00	-.171E+01	-.800E-04
19	.108E+00	-.199E+01	-.141E+00	-.171E+01	-.781E-04
20	.114E+00	-.199E+01	-.139E+00	-.172E+01	-.771E-04
21	.120E+00	-.200E+01	-.138E+00	-.172E+01	-.768E-04
22	.126E+00	-.200E+01	-.139E+00	-.172E+01	-.770E-04
23	.132E+00	-.200E+01	-.139E+00	-.172E+01	-.774E-04
24	.138E+00	-.200E+01	-.140E+00	-.172E+01	-.778E-04
25	.144E+00	-.201E+01	-.141E+00	-.172E+01	-.781E-04
26	.150E+00	-.201E+01	-.141E+00	-.172E+01	-.783E-04
27	.156E+00	-.201E+01	-.141E+00	-.172E+01	-.781E-04
28	.162E+00	-.200E+01	-.140E+00	-.172E+01	-.778E-04
29	.168E+00	-.200E+01	-.139E+00	-.172E+01	-.774E-04
30	.174E+00	-.200E+01	-.139E+00	-.172E+01	-.770E-04
31	.180E+00	-.200E+01	-.138E+00	-.172E+01	-.768E-04
32	.186E+00	-.199E+01	-.139E+00	-.172E+01	-.771E-04
33	.192E+00	-.199E+01	-.141E+00	-.171E+01	-.781E-04
34	.198E+00	-.200E+01	-.144E+00	-.171E+01	-.800E-04
35	.204E+00	-.200E+01	-.149E+00	-.170E+01	-.829E-04
36	.210E+00	-.200E+01	-.156E+00	-.169E+01	-.868E-04
37	.216E+00	-.201E+01	-.166E+00	-.168E+01	-.919E-04
38	.222E+00	-.201E+01	-.176E+00	-.165E+01	-.979E-04
39	.228E+00	-.200E+01	-.188E+00	-.163E+01	-.104E-03
40	.234E+00	-.199E+01	-.200E+00	-.159E+01	-.111E-03
41	.240E+00	-.196E+01	-.211E+00	-.154E+01	-.117E-03
42	.246E+00	-.191E+01	-.221E+00	-.147E+01	-.122E-03
43	.252E+00	-.184E+01	-.226E+00	-.139E+01	-.125E-03
44	.258E+00	-.173E+01	-.226E+00	-.128E+01	-.125E-03
45	.264E+00	-.159E+01	-.218E+00	-.116E+01	-.121E-03

```
46  .270E+00 -.141E+01 -.202E+00 -.101E+01 -.112E-03
47  .276E+00 -.119E+01 -.177E+00 -.835E+00 -.981E-04
48  .282E+00 -.923E+00 -.141E+00 -.642E+00 -.781E-04
49  .288E+00 -.624E+00 -.947E-01 -.434E+00 -.526E-04
50  .294E+00 -.301E+00 -.412E-01 -.218E+00 -.229E-04
51  .300E+00  .235E-01  .160E-01 -.863E-02  .891E-05
```

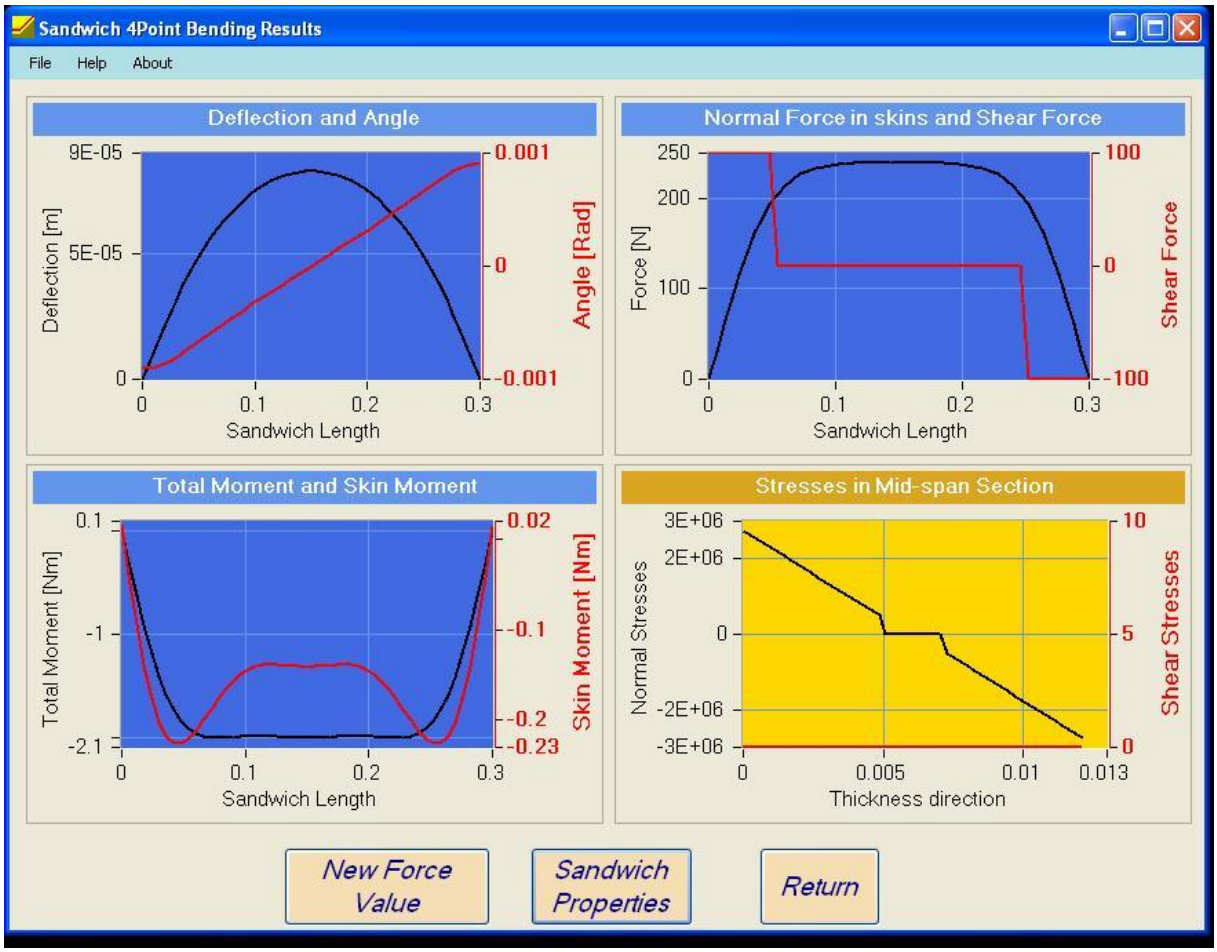

Figure 4.3.2.1 Graphical representation results 4-Point bending

4.3.3 Output File: c:\Ident_net\Geom_Files\Output_4P.CSV

All the results of the computations are also stored in a CSV File for further processing using the MS program EXCELL.

4.4 Identification of the transverse shear modulus

The program ***Sandwich_Resonalyser.exe*** can identify the transverse shear modulus of a sandwich beam based on the measurement of the frequency of the first bending mode. The Young's modulus of the skin and the Young's modulus of the core are assumed to be known (They can be measured using the Resonalyser on a skin material beam and a core material beam)

4.4.1 Input File: c:\Ident_net\Geom_Files\Shearident_Input.txt

read(2,*)BLENGTH	Length of the beam [m]
read(2,*)BWIDTH	Width of the beam [m]
read(2,*)H	Skin thickness [m]
read(2,*)H0	Core thickness [m]
read(2,*)RHO	Skin density [kg/m3],
read(2,*)RHO0	Core density [kg/m3]
read(2,*)EGLAS	Young 's Modulus skin [kg/m3]
read(2,*)EPOLY	Young 's Modulus core [kg/m3]
read(2,*)GPOLY	Transverse shear modulus [Pa]
read(2,*) FREQMEAS	Measured bending frequency beam [Hz]
read(2,*)KODAC	Accelerometer node position
read(2,*)ACCELM	Accelerometer mass

Example input File

```
0.3000000
0.0300000
0.0049300
0.0012800
2.473E+03
1.100E+03
7.1000E+10
2.000E+08
585.60
5
0.0
```

4.4.2 Output File: c:\Ident_net\Geom_Files\Shearident_Output.txt

```
*****************************************************************************
*
*             IDENTIFICATION OF SHEAR MODULUS
*
*****************************************************************************


*****************************************************************************
*
*             INPUT SECTION
*
*****************************************************************************
```

```
&&&  CONTROL INFORMATION

          NUMBER OF NODAL POINTS    :        11


     &&& BEAM PROPERTIES :


          Length Beam       :              .30000
          Width  Beam       :             3.00000E-02
          Thick skin layer  :             4.93000E-03
          Thick Poly layer  :             1.28000E-03
          Specific Mass skin :             2473.0
          Specific Mass Poly :             1100.0
          Beam Mass         :             .23213
          E-modulus skin    :             7.10000E+10
          E-modulus Poly    :             2.00000E+08
          Measured Frequency :               585.60
          Accelerometer Node :              5
          Accelerometer Mass:               .00000



*************************************************************************
*
*               RESULTS
*
*************************************************************************


     &&&  EIGENVALUE SPECIFICATIONS


          NUMBER OF EIGENFREQUENCIES    :      1
          LOWER LIMIT EIGENFREQUENCIES  :      292.80
          HIGHER LIMIT EIGENFREQUENCIES :      704.36


     &&& START VALUES :


          Freq measured      :             585.60
          Minimal Freq  :                  292.80
          Maximal Freq  :                  704.36
          EI-Max:                        245.02
          Shear Poly :                    6.89655E+07
          Young Modulus Poly       :      2.00000E+08


*************************************************************************
*
*               OUTPUT SECTION
*
*************************************************************************



*************
 BISECTIONS
*************

FREQMI start =     292.799987792968800
FREQMA start=     704.357981575640700
CHECKNORM =   9.998256203784608E-001

ITER =         1
FREQMI after eigenvalue computation =     539.375564454338800
FREQMA after eigenvalue computation =     627.314181945437700
FREQ Measured =     585.599975585937500
```

```
FREQ Numerical =      611.767304962198400
GPOLY =   6.896551497342619E+007
STARTLOW =          1
FREQMI start =      292.799987792968800
FREQMA start=      704.357981575640700
CHECKNORM =   9.997008146925499E-001

ITER =          2
FREQMI after eigenvalue computation =      539.375564454338800
FREQMA after eigenvalue computation =      627.314181945437700
FREQ Measured =      585.599975585937500
FREQ Numerical =      558.907249521375100
GPOLY =   3.448275748671310E+007
STARTHI =          1

************************
 RESULT AFTER BISECTIONS
************************

GPOLYMI =   3.448275748671310E+007
GPOLYMA =   6.896551497342619E+007
FREQ MI =      558.907248724924800
FREQ ma =      611.767296924919600

*****************************
 RESULTS AFTER INTERPOLATION
*****************************

GPOLY  AFTER INTERPOLATION =  5.150629211121322E+007

FREQ Measured =      585.600000
FREQ Numeriek =      591.218333975115100

************************
 DURING STRESS ITERATION
************************

GPOLY DURING STRESS ITERATION NR.          1  =  4.766262053081347E+007
FREQ Numerical =      585.317646769933100
FREQ Measured =      585.599975585937500
Percentage Convergence =    9.640054E-02

GPOLY DURING STRESS ITERATION NR.          2  =  4.783692905917811E+007
FREQ Numerical =      585.599340351143800
FREQ Measured =      585.599975585937500
Percentage Convergence =    2.169517E-04


************************************
 FINAL RESULTS AFTER STRESS ITERATION
************************************

GPOLY AFTER STRESS ITERATION =  4.783732312591564E+007
FREQ Numerical =      585.599340351143800
FREQ Measured =      585.599975585937500
The sensitivity of lambda for G =   7.453342009492166E-002
The relative sensitivity Lambda for G =   2.633638018322094E-001
The percentage change of Lambda ERRORL =   2.000000029802322E-001
The percentage change of G for ERRORL =   7.594058165504970E-001


COMPUTATION OF THE MAXIMAL POSSIBLE SANDWICH FREQUENCY
******************************************************

FINAL VALUE GPOLY =  4.783732312591564E+007
FINAL VALUE POISSON POLY = 0.45
FINAL VALUE EPOLY =  1.387282416272780E+008

          APPARENT BEAM STIFFNESS VALUE:           169.36
          MAXIMAL CLT BEAM STIFFNESS:             243.32
          SANDWICH STIFFNESS PER METER:            5645.3
```

```
MAXIMAL SANDWICH STIFFNESS PER METER:      8110.6

COMPUTED SANDWICH FREQUENCY:            585.60
MEASURED SANDWICH FREQUENCY:            585.60
MAXIMAL POSSIBLE SANDWICH FREQUENCY:      701.91

COMPUTATION OF THE POTENTIAL AND KINETIC ENERGY
***********************************************

TOTAL POTENTIAL ENERGY:              6.76911E+06
CONTRIBUTION BENDING MOMENT:            1.76834E+06
CONTRIBUTION NORMAL FORCE:           3.21802E+06
CONTRIBUTION SHEAR FORCE:            1.78272E+06
CONTRIBUTION BENDING CORE:             30.237


TOTAL KINETIC ENERGY:                6.76911E+06
CONTRIBUTION MASS:                   6.74399E+06
CONTRIBUTION INERTIA:                  25123.
```

The graphical output for a measured damping ratio of 1.515% is:

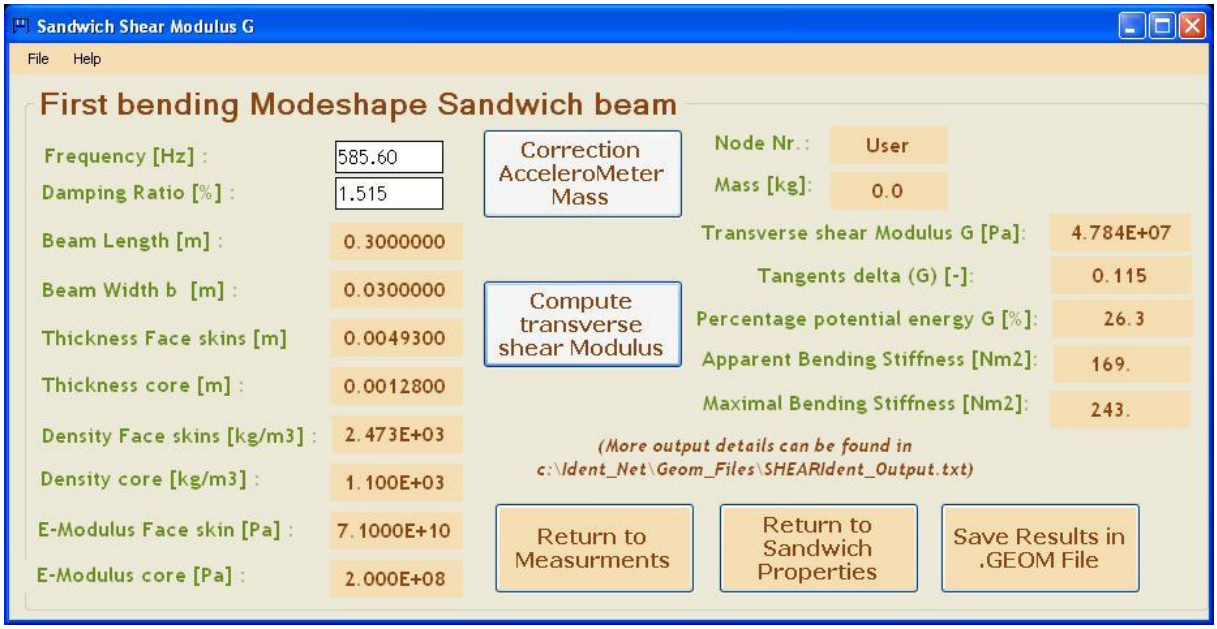

Figure 4.4.2.1 Graphical output identification results

4.5 Identification with variable thickness

The program ***Sandwich_VarThick.exe*** can identify the transverse shear modulus of a sandwich beam based on the measurement of the frequency of the first bending mode. The Young's modulus of the skin and the Young's modulus of the core are assumed to be known (They can be measured using the Resonalyser on a skin material beam and a core material beam). The thickness of the PVB layer can vary in each nodal point of the numerical modal.

4.5.1 Input File: c:\Ident_net\Geom_Files\Var_Shear_Input.txt

```
      read(2,*)BLENGTH      Length of the sandwich beam
      read(2,*)BWIDTH       Width of the sandwich beam
      read(2,*)H            Thickness of the skin layer
      read(2,*)RHO          Density of the skin layer
      read(2,*)RHO0         Density of the inner layer
      read(2,*)EGLAS        Young's modulus of the skin
      read(2,*)EPOLY        Young's modulus of the core
      read(2,*)FREQMEAS     Measured resonance frequency
      read(2,*)KODAC        Node position of the accelerometer
      read(2,*)ACCELM       Accelerometer mass

      NNODE=11
      DO 10 I=1,NNODE
            read(2,*)H0(I)  Thickness of the core layer in Node I
10    CONTINUE
```

Example input File:

```
0.3000000
0.0302000
0.0049430
2.475E+03
1.065E+03
7.0900E+10
4.231E+08
676.00
5
0.0

0.002179
0.002191
0.002206
0.002221
0.002233
0.002236
0.002191
0.002166
0.002065
0.001967
0.001884
```

4.5.2 Output File: c:\Ident_net\Geom_Files\Var_Shear_Output.txt

```
*****************************************************************************
*
*              IDENTIFICATION OF SHEAR MODULUS
*
*****************************************************************************


*****************************************************************************
*
*              INPUT SECTION
*
*****************************************************************************


     &&&  CONTROL INFORMATION

          NUMBER OF NODAL POINTS    :         11


     &&& BEAM PROPERTIES :


          Length Beam       :              .30000
          Width  Beam       :             3.02000E-02
          Thick skin layer  :             4.94300E-03
          Specific Mass skin :             2475.0
          Specific Mass Poly :             1065.0
          Beam Mass         :             .24243
          E-modulus skin    :             7.09000E+10
          E-modulus Poly    :             4.23100E+08
          Measured Frequency :              676.00
          Accelerometer Node :             5
          Accelerometer Mass:               .00000


     &&& CORE LAYER THICKNESS :


          Node 1       :              2.17900E-03
          Node 2       :              2.19100E-03
          Node 3       :              2.20600E-03
          Node 4       :              2.22100E-03
          Node 5       :              2.23300E-03
          Node 6       :              2.23600E-03
          Node 7       :              2.19100E-03
          Node 8       :              2.16600E-03
          Node 9       :              2.06500E-03
          Node 10      :              1.96700E-03
          Node 11      :              1.88400E-03
```

```
*****************************************************************************
*
*              RESULTS
*
*****************************************************************************


     &&&  EIGENVALUE SPECIFICATIONS


          NUMBER OF EIGENFREQUENCIES    :      1
          LOWER LIMIT EIGENFREQUENCIES  :      338.00
          HIGHER LIMIT EIGENFREQUENCIES :      782.25


     &&& START VALUES :


          Freq measured      :             676.00
          Minimal Freq  :                  338.00
          Maximal Freq  :                  782.25
          EI-Max:                        315.62
          Shear Poly :                    1.45897E+08
          Young Modulus Poly       :      4.23100E+08


*****************************************************************************
*
*              OUTPUT SECTION
*
*****************************************************************************



*************
 BISECTIONS
*************

FREQMI start =     338.000000000000000
FREQMA start=     782.248270199119100
CHECKNORM =   9.998235397032244E-001

ITER =         1
FREQMI after eigenvalue computation =     602.559688424936900
FREQMA after eigenvalue computation =     698.208612931791000
FREQ Measured =     676.000000000000000
FREQ Numerical =     687.514396085298000
GPOLY =   1.458965469262831E+008
STARTLOW =          1
FREQMI start =     338.000000000000000
FREQMA start=     782.248270199119100
CHECKNORM =   9.995669126949196E-001

ITER =         2
FREQMI after eigenvalue computation =     602.559688424936900
FREQMA after eigenvalue computation =     698.208612931791000
FREQ Measured =     676.000000000000000
FREQ Numerical =     630.940436863140800
GPOLY =   7.294827346314156E+007
STARTHI =          1
```

****
RESULT AFTER BISECTIONS
****

GPOLYMI = 7.294827346314156E+007
GPOLYMA = 1.458965469262831E+008
FREQ MI = 630.940440248734600
FREQ ma = 687.514390758515600

****
RESULTS AFTER INTERPOLATION
****

GPOLY AFTER INTERPOLATION = 1.305421082180432E+008

FREQ Measured = 676.000000
FREQ Numeriek = 679.652795547190600

****
DURING STRESS ITERATION
****

GPOLY DURING STRESS ITERATION NR. 1 = 1.240121506907743E+008
FREQ Numerical = 675.864010502507100
FREQ Measured = 676.000000000000000
Percentage Convergence = 4.022953E-02

GPOLY DURING STRESS ITERATION NR. 2 = 1.242376165074655E+008
FREQ Numerical = 675.999853276899000
FREQ Measured = 676.000000000000000
Percentage Convergence = 4.340920E-05

****
FINAL RESULTS AFTER STRESS ITERATION
****

GPOLY AFTER STRESS ITERATION = 1.242378604079602E+008
FREQ Numerical = 675.999853276899000
FREQ Measured = 676.000000000000000
The sensitivity of lambda for G = 3.210775221794490E-002
The relative sensitivity Lambda for G = 2.211111980127653E-001
The percentage change of Lambda ERRORL = 2.000000029802322E-001
The percentage change of G for ERRORL = 9.045222710461085E-001

COMPUTATION OF THE MAXIMAL POSSIBLE SANDWICH FREQUENCY
****

FINAL VALUE GPOLY = 1.242378604079602E+008
FINAL VALUE POISSON POLY = 0.45
FINAL VALUE EPOLY = 3.602898070313303E+008

APPARENT BEAM STIFFNESS VALUE: 235.70
MAXIMAL CLT BEAM STIFFNESS: 311.02
SANDWICH STIFFNESS PER METER: 7804.8
MAXIMAL SANDWICH STIFFNESS PER METER: 10299.

COMPUTED SANDWICH FREQUENCY: 676.00
MEASURED SANDWICH FREQUENCY: 676.00
MAXIMAL POSSIBLE SANDWICH FREQUENCY: 776.52

COMPUTATION OF THE POTENTIAL AND KINETIC ENERGY
****

TOTAL POTENTIAL ENERGY:	9.02034E+06
CONTRIBUTION BENDING MOMENT:	1.71234E+06
CONTRIBUTION NORMAL FORCE:	5.31312E+06
CONTRIBUTION SHEAR FORCE:	1.99449E+06
CONTRIBUTION BENDING CORE:	390.52
TOTAL KINETIC ENERGY:	9.02885E+06
CONTRIBUTION MASS:	8.98414E+06
CONTRIBUTION INERTIA:	44717.

The graphical output for a measured damping ratio of 4.330 % is:

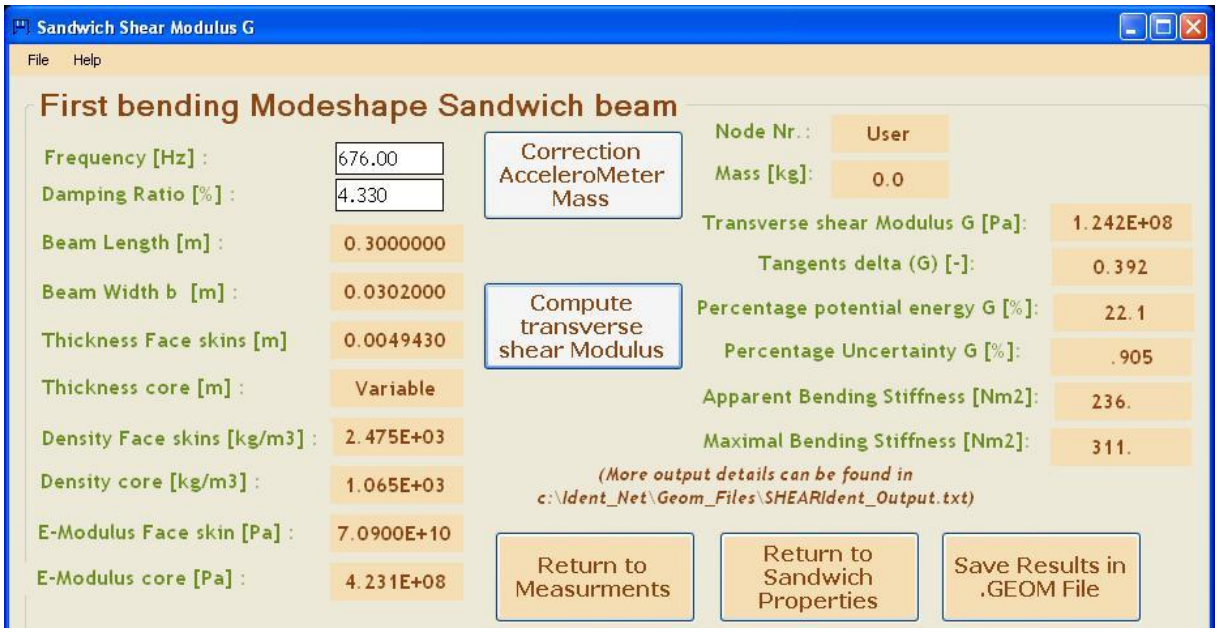

Figure 4.5.2.1 Graphical output identification results

5 Discussion

Within the limits of the model assumptions, the simulation results are correct. The main assumptions are linearity and constant shear stress in the middle layer.

The identification results based on experimental measurements not only rely on the numerical model, but also on the **quality of the input** date:

- The correct Young's modulus of the glass layer
- The correct density of glass and PVB
- The real thickness of both glass layers
- The width and correct alignment of both glass layers
- The correct length of both glass layers
- The correct thickness profile of the middle layer
- Homogeneity of the PVB layer (can be reached if proper pre-curing with controlled temperature and humidity is long enough applied e.g. at least during 24 hours before measurement)

The resonance frequency of an ***assumed perfect model*** with correct input data can differ from the measured resonance frequency of the real physical model with real uncertainties on the input data.

The identification results also rely on the correctness of the measured quantities (resonance frequencies and modal damping ratios)

The Impulse excitation technique measures the decaying signal after an impact on a freely suspended test beam. The decaying signal is sampled in the time domain and converted to the frequency domain by Fast Fourier transformation. The sample rate is chosen in such a way that the identification of the resonance frequencies is better than 0.1% accuracy.

The resonance frequency is the result of constant transformation of potential energy into kinetic energy and vice versa. Both energy quantities are big enough to allow accurate measurement of the time signal with an accelerometer without necessity of high signal amplification.

The value of the damping energy is much lower than the value of the potential and kinetic energy. Damping measurements are therefore less accurate. The damping ratio can also behave non-linear as a function of the vibration amplitude. Damping measurements hence can be more cumbersome than measurements of resonance frequencies.

If the test beam shows a lightly damped resonance frequency, the damping ratio can be found accurately by curve fitting the decaying signal in the time domain. Higher damping can better be identified with the 3DB rule in the frequency domain. Damping also often behaves non linear and dependant on force of the excitation and the amplitude of the decaying signal.

It is critical that the accelerometer is fixed accurately in the middle of the test beam. This allows the simulation of mass of the accelerometer in the numerical model as a concentrated mass in the middle nodal point. The mass of the accelerometer wires must also be taken into account in the mass loading.

The test beam must be suspended at the positions of 0.224 times the length away from the extreme ends of the beam. In this way the suspensions wires are fixed in a zero amplitude position of the vibration associated with the first bending modal shape and hence disturb minimal the vibration.

The Resonalyser equipment used for the validation in this report allows measuring the resonance frequency with 0.1% accuracy and the damping ratio typically with 5% accuracy. In a perfect world, this allows a good identification of the transverse shear storage modulus and tangents delta.

However, samples do not satisfy all the above mentioned specification for a perfect quality. In reality this can cause a few Hertz difference between the measured resonance frequency and what would be the resonance frequency of a perfect sample. So an important question is “how doe small deviations of the resonance frequency and damping ratio influence the identified result? The answer of this question relies on the **sensitivity** of the identified transverse shear values for small variations of the frequency and modal damping. The sensitivity value is low in both the extreme regions in figure 3.3.1:

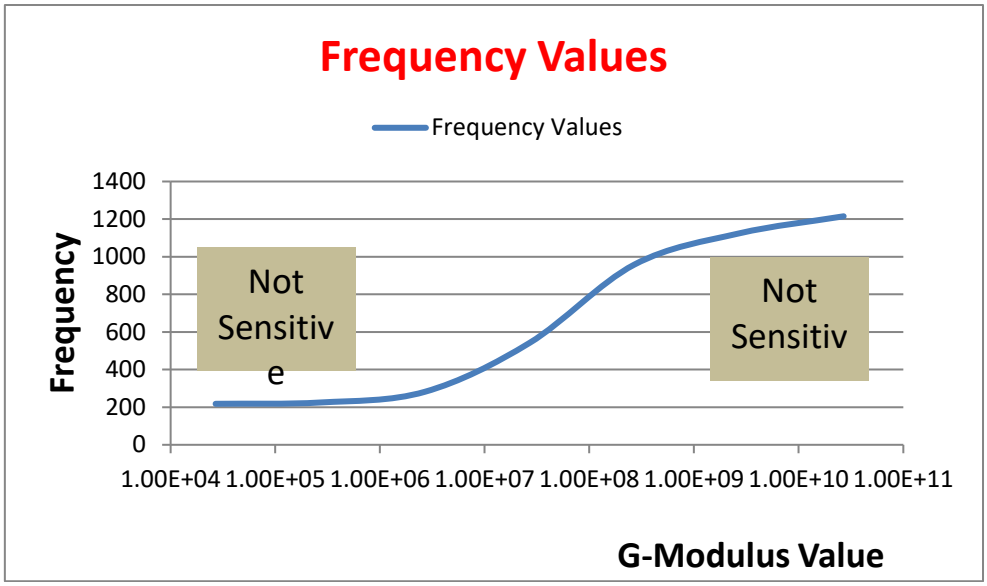

Figure 3.3.1 influence of G modulus on the resonance frequency

Example 1: non-sensitive right region of figure 3.3.1 (high G-values)

Thickness glass layers: 4.93 mm
Thickness PVB layer: 1.28 mm
Width test beam: 0.03 m
E-Modulus glass: 71 GPa
Poisson ratio glass: 0.23
Density glass: 2473 kg/m3
Density PVB: 1100 kg/m3

Case	Freq. F [Hz]	Damping Ratio [%]	Storage Modulus G [MPa]	Tangents Delta [-]	Uncertainty Storage G [%]	Relative Sensitivity ΔF/ΔG	Identif. storageG [MPa]	Identif. Tangent [-]
1	692.4	0.54	843	0.4644	7.515	0.026	889.4	0.406
	691.4	0.54	843	0.4644	6.816	0.026	802.2	0.368
	693.4	0.54	843	0.4644	8.34	0.026	997.0	0.452
	692.4	0.64	843	0.4644	7.515	0.026	889.4	0.481

Table 5.1 influence of G modulus on the resonance frequency

The relative sensitivity is low. The above results show that only 1 Hz difference on the input value of the resonance frequency cause about 7% difference on the value of the identified storage modulus. This means that even nearly perfect input values cause dramatic difference in the result. Thus indeed, the right zone of figure 3.3.1 is not suitable for identification. The sandwich beam behaves as a classical laminate with very little influence of transverse shear deformation.

Example 2: middle region of figure 3.3.1 (average G-values)
(Same geometry as previous case)

Case	Freq. F [Hz]	Damping Ratio [%]	Storage Modulus G [MPa]	Tangents Delta [%]	Uncertainty Storage G [%]	Relative Sensitivity ΔF/ΔG	Identif. storageG [MPa]	Identif. Tangent [%]
2	585.6	1.515	47.89	0.1149	0.759	0.26	47.84	0.115
	584.6	1.515	47.89	0.1149	0.754	0.26	47.24	0.114
	586.6	1.515	47.89	0.1149	0.764	0.26	48.46	0.116
	585.6	1.415	47.89	0.1149	0.759	0.26	47.84	0.108

Table 5.2 influence of G modulus on the resonance frequency

The relative sensitivity is 10 times higher than the previous case. The above result shows that small variations on the frequencies and damping ratio only yield small variations in the identified results. This shows that the middle section of 3.3.1 is a stable zone for identification.

Example 3: non-sensitive left region of figure 3.3.1 (low G-values)
(Same geometry as previous case)

Case	Freq. F [Hz]	Damping Ratio [%]	Storage Modulus G [MPa]	Tangents Delta [%]	Uncertainty Storage G [%]	Relative Sensitivity ΔF/ΔG	Identif. StorageG [MPa]	Identif. Tangent [%]
3	295.9	5.0	0.1	5.50	10.973	0.018	0.099	5.485
	296.9	5.0	0.1	5.50	8.078	0.018	0.136	4.039
	294.9	5.0	0.1	5.50	17.232	0.018	0.062	8.613
	295.9	4.0	0.1	5.50	10.973	0.018	0.099	4.388

Table 5.3 influence of G modulus on the resonance frequency

The relative sensitivity is 10 times lower than the previous case. The above results show that only 1 Hz difference on the input value of the resonance frequency cause more than 10% difference on the value of the identified storage modulus. This means that even nearly perfect input values cause dramatic difference in the result. Thus indeed, the left zone of figure 3.3.1 is not suitable for identification.

The discussion about a good value of the sensitivity of the resonance frequencies for changes of transverse shear modulus is not straight forward. The best indication is the uncertainty of the storage modulus. If this value is higher than 5%, the result for the identified storage modulus is unstable.

The value of the **tangents delta** is dependent on the correct identification of the potential energy computations and the correct value of the measured damping ratio.

6 Conclusion

There are two important origins of the uncertainty of the identified transverse shear modulus using the numerical model and the impulse excitation technique:

- Imperfections of the test beams geometry and errors in the values of the input data on material properties (Young's modulus of the glass, density values).
- The sensitivity of the resonance frequencies for variations of the transverse shear values. There are two clearly regions with low sensitivity: regions with very high value of the transverse shear storage modulus (classical laminate theory with nearly no influence of transverse shear deformations) and regions with a very low value of the transverse shear modulus (independent bending of the skin slayers)

The influence of measurement errors with the impulse excitation technique can be neglected as compared with the above considerations (0.1% error on the measured resonance frequencies and 5% error on the measured modal damping ratios).

The accuracy of the numerical model is good within the limits of the assumption of linearity and constant shear stress in the core layer (hence sufficient low thickness of the core layer).